

國立交通大學

光電工程研究所

碩士論文

延展高分子分散型液晶在散射式偏光膜之應用



Optical Properties of Stretched PDLC films for
Scattering Polarizer Applications

研究生：邱浩瑋

指導教授：謝漢萍 教授

田仲豪 助理教授

中華民國九十七年七月

延展高分子分散型液晶在散射式偏光膜之應用

Optical Properties of Stretched PDLC films for
Scattering Polarizer Applications

研 究 生：邱浩璋

Student：Hao-Wei Chiu

指 導 教 授：謝漢萍

Advisor：Dr. Han-Ping D. Shieh

田仲豪

Dr. Chung-Hao Tien

國立交通大學



Submitted to Institute of Electro-Optical Engineering

College of Electrical Engineering and Computer Science

National Chiao-Tung University

in Partial Fulfillment of the Requirements

for the Degree of Master

in

Electro-Optical Engineering

July 2008

Hsinchu, Taiwan, Republic of China

中華民國九十七年七月

延展高分子分散型液晶在 散射式偏光膜之應用

研究生：邱浩璋 指導教授：謝漢萍 教授

田仲豪 助理教授

國立交通大學光電工程研究所



傳統吸收式偏光片為液晶顯示器中主要元件之一，然而，穿透式液晶顯示器由於吸收式偏光片、濾光片、導光板…等元件吸收而光利用效率低落。近年來，非吸收式偏光片由於具有將原本應被吸收的光回收利用的特性而受到廣泛注目和研究，非吸收式偏光片的工作原理主要分為反射式和散射式兩大類，而能將光反射或散射之後回收利用。

具有極化選擇性的延展高分子分散型液晶薄膜為散射式偏光片的一種，應用於液晶顯示器中，可有效地將光散射回背光模組中並回收利用，而提升光效率，達到增亮的效果。本篇論文的主要目的便是研究延展高分子分散型液晶薄膜的光學特性，並將拉伸方向由一維單向進一步地延伸至二維徑向拉伸，製作徑向對稱偏光片。

Optical Properties of Stretched PDLC Films for Scattering Polarizer Applications

Student : Hao-Wei Chiu

Advisor : Dr. Han-Ping D. Shieh

Dr. Chung-Hao Tien

Institute of Electro-Optical Engineering
National Chiao Tung University



The conventional absorbing polarizer is a key component in current LCDs. However, the optical efficiency of typical transmission type LCDs was low due to absorbing polarizer, color filter, light guide in back light module, and so on. Recently, nonabsorbing polarizers were widely noticed to recycle the light utilization. The basic concepts of nonabsorbing polarizers fall into two categories: reflecting and scattering.

The stretched PDLC film associated with polarization selectivity is a sort of scattering polarizer. With this film utilized in LCDs, the light is backscattered and recycled in the backlight module instead of being absorbed. The light efficiency was thus enhanced by polarization recycling mechanism. The purpose of this thesis was to investigate the optical properties of the stretched PDLC films. In conclusion, the fabricated film performed 50% transmittance along transmission axis and 0.06 for extinction ratio. Besides, the direction of polarization of the converted light can be controlled by varying the stretching direction of the films. The azimuthal polarizers are fabricated by change the stretching direction from linear to two-dimensional radially direction.

誌謝

在論文完成的此刻，雖然我的碩士班研究生活比較長，但終究到了這個感傷的離別時候。在交大光電所的期間，無論在學業上或生活上都學習到許多，最要感謝的是在這段時間裡細心指導、鼓勵我的謝漢萍教授和田仲豪教授及光資訊系統實驗室優良的研究環境；記得在研究過程中，有時覺得自己不適應研究所的學習方式，遭遇挫折，但在兩位老師的指導下，學業漸漸上了軌道，讓我藉由參與計畫的實驗過程中，獲益良多。

其次要感謝在這段期間陪伴我的學長姊、同學和學弟妹們，讓我的生活更加多采多姿，並在學業上給我許多指導、鼓勵與支持。還要特別感謝陳皇銘教授對我論文的悉心指導，以及實驗夥伴方廷綺在實驗合作過程中對我的一切幫助。

最後我要感謝我的家人和女友在一路上給我的支持與陪伴，讓我度過一切的低潮，使我能順利完成學業，僅將本文獻給家人與關心我的人們。

Table of Contents

Abstract (Chinese)	i
Abstract (English)	ii
Table of Contents	iv
Figure Caption	vi
Table Caption	ix
Chapter 1 Introduction	1
1.1 Preface	1
1.2 Optical Films in the Backlight Module	2
1.2.1 Diffuser	3
1.2.2 Brightness Enhancement Films (BEF)	4
1.3 Polarizer	5
1.3.1 Absorbing Polarizer	5
1.3.2 Reflecting Polarizer	7
1.3.3 Scattering Polarizer	10
1.4 Motivation and Objective	11
1.5 Organization of This Thesis	11
Chapter 2 Principle	12
2.1 Polarization of Optical Waves	12
2.2 Spatially Inhomogeneous Polarized Beam	17
2.2.1 Cylindrical Vector Beam	17
2.3 Polymer-dispersed Liquid Crystals (PDLC)	19
2.3.1 PDLC Light Modulator	19

2.3.2 Elongation of Liquid Crystal Droplets -----	22
2.3.3 One-dimensional Linearly Stretched PDLC Film -----	24
2.3.4 Two-dimensional Radially Stretched PDLC Film -----	26
Chapter 3 Fabrication and Measurement Instruments -----	28
3.1 Preparation of Stretched PDLC Films -----	28
3.1.1 Fabrication of PDLC Films -----	28
3.1.2 Real-time Measurement Set-up of Optical Properties -----	31
3.1.3 Radially Stretching Process -----	32
3.2 FT-IR Spectrometer -----	33
Chapter 4 Experimental Results and Discussion -----	36
4.1 Introduction-----	36
4.2 Optical Properties of Stretched PDLC Films -----	36
4.2.1 Elongated LC Droplets in Stretched PDLC Films -----	36
4.2.2 Dependence of LC Concentration on Optical Properties-----	38
4.2.3 Effect of Relative Humidity during Drying Process -----	40
4.2.4 Dependence of Film Thickness on Optical Properties -----	42
4.3 Ordering Parameter of Liquid Crystal -----	44
4.4 Function of Azimuthal Polarizer -----	44
4.5 Discussion -----	46
Chapter 5 Conclusion and Future Work -----	48
5.1 Conclusion -----	48
5.2 Future Works -----	49

Figure Caption

Fig. 1 Comparison between various polarizers used in LCDs : (a) absorbing polarizer (b) reflecting polarizer (c) scattering polarizer -----	2
Fig. 2 Conventional backlight module with (a) two sheets of prismatic films crossed at 90° (b) single sheet of prismatic film and reflecting polarizer -----	3
Fig. 3 BEF with pitch of 50 μm and prism angle fixed 90° -----	4
Fig. 4 On-axis intensity enhancement of the BLM with BEFs -----	5
Fig. 5 Dichroic polarizer in LCD Displays -----	6
Fig. 6 Transmission and absorption axes of dichroic linear polarizer -----	7
Fig. 7 DBEF with multilayer structures -----	8
Fig. 8 LCD display enhanced by DBEF -----	8
Fig. 9 The mechanism of the reflecting polarizer based on a cholesteric film with a quarter wave plate -----	9
Fig. 10 A scattering polarizer based on PDLC technology -----	10
Fig. 11 Light linearly polarized (a) in the first and third quadrants ($\delta = 0$) (b) in the first and third quadrants ($\delta = \pm\pi$) oscillating in time -----	13
Fig. 12 (a) Right-hand circularly polarized light with the electric field rotating clockwise (b) left-hand circularly polarized light with the electric field rotating counterclockwise -----	14
Fig. 13 Elliptically polarized light -----	16
Fig. 14 Elliptical polarization configuration at various relative phase difference δ when (a) $E_{0y} = E_{0x}$ and (b) $E_{0y} > E_{0x}$ -----	16
Fig. 15 (a) The spatially homogeneous polarized beam and (b) the spatially inhomogeneous polarized beam -----	18

Fig. 16 The field distribution of the cylindrical vector beams (a) radially polarized beam and (b) azimuthally polarized beam where the arrows represent the polarization	19
Fig. 17 Polymer dispersed liquid crystal (PDLC) light modulator	20
Fig. 18 The scattering mechanism of the PDLC operation. (a) Off-state (b) On-state – viewing at the normal (c) On-state – viewing off-axis	22
Fig. 19 Technique of elongating liquid crystal droplets (a) Stretching of PDLC film (b) deforming effect of electric field (c) shearing of system	24
Fig. 20 PDLC films (a) before and (b) after stretching	25
Fig. 21 The refraction index difference in the stretched PDLC films	25
Fig. 22 Mechanism of a scattering polarizer based on PDLC technology	26
Fig. 23 Mechanism of a azimuthal polarizer by radially stretching of PDLC film ---	27
Fig. 24 Flow of preparation of PDLC films (a) the emulsion applied on the PET substrate (b) Meyer Bar coating (c) the film dried in sweatbox (d) the film one-dimensionally stretched by micro-tensile tester	30
Fig. 25 Schematic representation of real-time measurement set-up	31
Fig. 26 The pictures of real-time measurement set-up	32
Fig. 27 Samples cut in the shape defined by ASTM standard D 1708	32
Fig. 28 The set-up of radially stretching process	33
Fig. 29 Inside layout of the FT-IR Spectrometer	34
Fig. 30 Polarized infrared spectra of a stretched PDLC film (PVA/E7) with the polarizations of the incident beam parallel and perpendicular to the stretching direction	35
Fig. 31 The PDLC films stretched under the strains of (a) 0% (unstretched) (b) 20% (c) 30% (d) 40% (e) 50% (f) 70%	37

Fig. 32 The strain-transmittance curve of the PDLC films with different concentration of E7-----	39
Fig. 33 The extinction ratio properties of the PDLC films with different concentration of E7 -----	40
Fig. 34 The strain-transmittance curve of the PDLC films dried under the condition of different relative humidity -----	41
Fig. 35 The extinction ratio properties of the PDLC films dried under the condition of different relative humidity -----	42
Fig. 36 The strain-transmittance curve of the PDLC films with different film thickness -----	43
Fig. 37 The extinction ratio properties of the PDLC films with different film thickness -----	43
Fig. 38 Definition of the strain in the radially stretching process -----	45
Fig. 39 The polarization testing set-up -----	46
Fig. 40 CCD images with (a) azimuthally polarized (b) radially polarized incident beam -----	46
Fig. 41 Schematic representation of (a) the typical orientation of the bipolar director configuration, and (b) the orientation of the bipolar configuration in an 'anomalous' droplet -----	47

Table Caption

Tab. 1 Comparison of state of polarization -----	17
Tab. 2 Refraction indices of E7 and PVA -----	29
Tab. 3 Strain and range of deformation of the stretched PDLC films -----	38
Tab. 4 Ordering parameter of liquid crystal under different strain -----	44
Tab. 5 Fabrication parameters of stretched PDLC films -----	48



Chapter 1

Introduction

1.1 Preface

The Polarizer is a device that converts an unpolarized light in liquid crystal displays (LCDs). Conventional dichroic polarizers based on absorption are iodine doped polyvinyl alcohol (PVA) films that transmit one polarization state and absorb the orthogonal component, therefore less than 50% of light can be utilized. In order to improve the light efficiency of LCDs, a polarization recycling technique has been proposed to use nonabsorbing polarizers. The basic concepts of nonabsorbing polarizers fall into two types: reflecting and scattering [1]. With a polarization recycling mechanism, the nonabsorbing polarizer efficiently reflects or backscatters light to the light guide, as shown in Fig. 1. In this study, the optical properties of stretched polymer dispersed liquid crystal (PDLC) film with polarization selectivity due to anisotropic scattering in a polymer matrix are analyzed. It is expected that stretched PDLC films as scattering polarizers are able to enhance the light efficiency in the backlight module of the LCD displays.

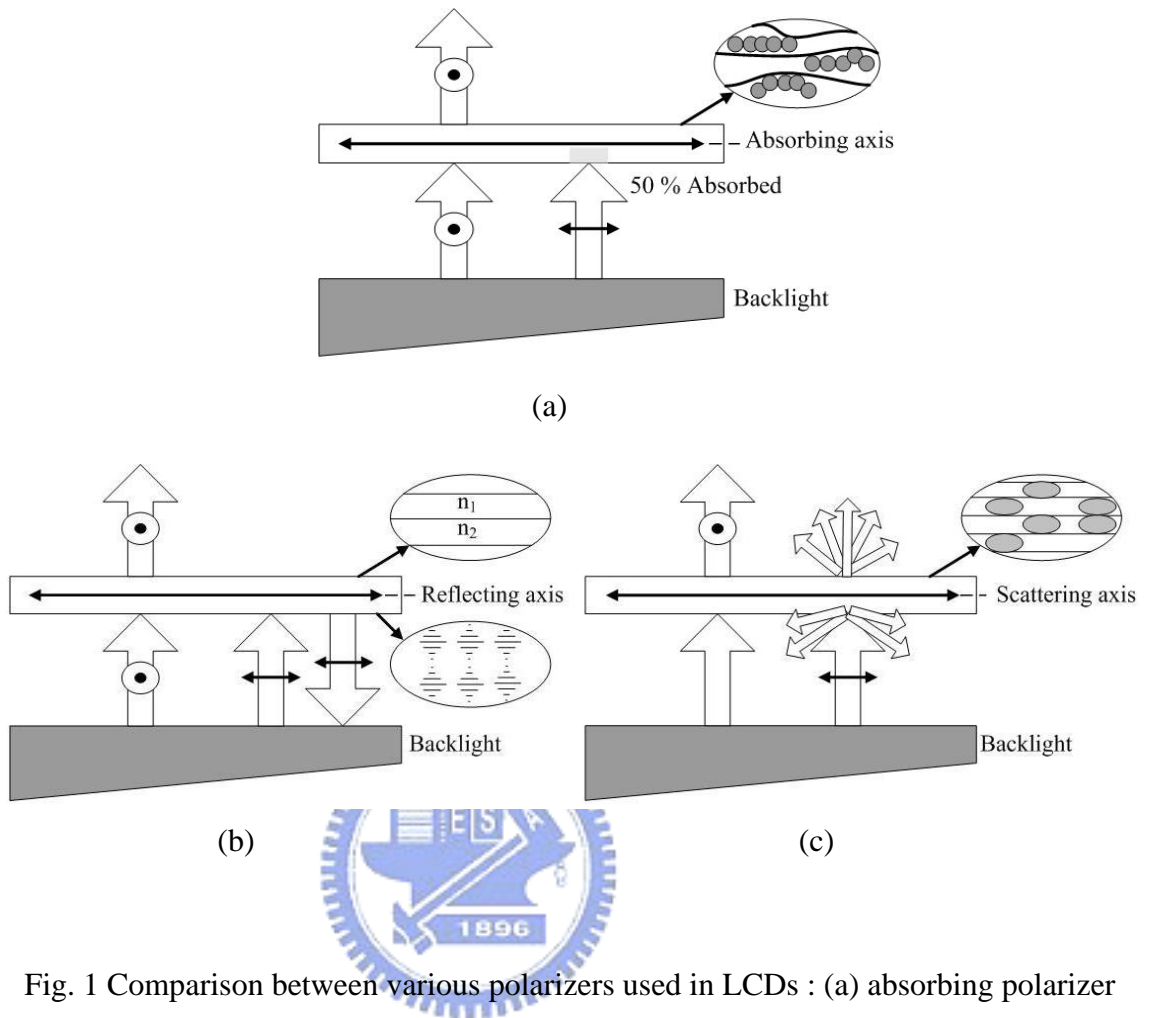


Fig. 1 Comparison between various polarizers used in LCDs : (a) absorbing polarizer
 (b) reflecting polarizer (c) scattering polarizer

1.2 Optical Films in the Backlight Module

The Backlight module (BLM) of LCD display is composed of light source, light guide and optical films. Conventional BLM is shown in Fig. 2. Light emitting from the light source transmits in the wedge type light guide. After extracting from the light guide, light enters the diffuser and is scattered into all directions of the upper space. The prismatic films redirect and collect the scattered light to the normal viewing direction. With the reflecting or scattering polarizer applied in the BLM, the brightness can be enhanced through polarization recycling. These optical films employed in the BLM

promote light uniformity, collimation and brightness.

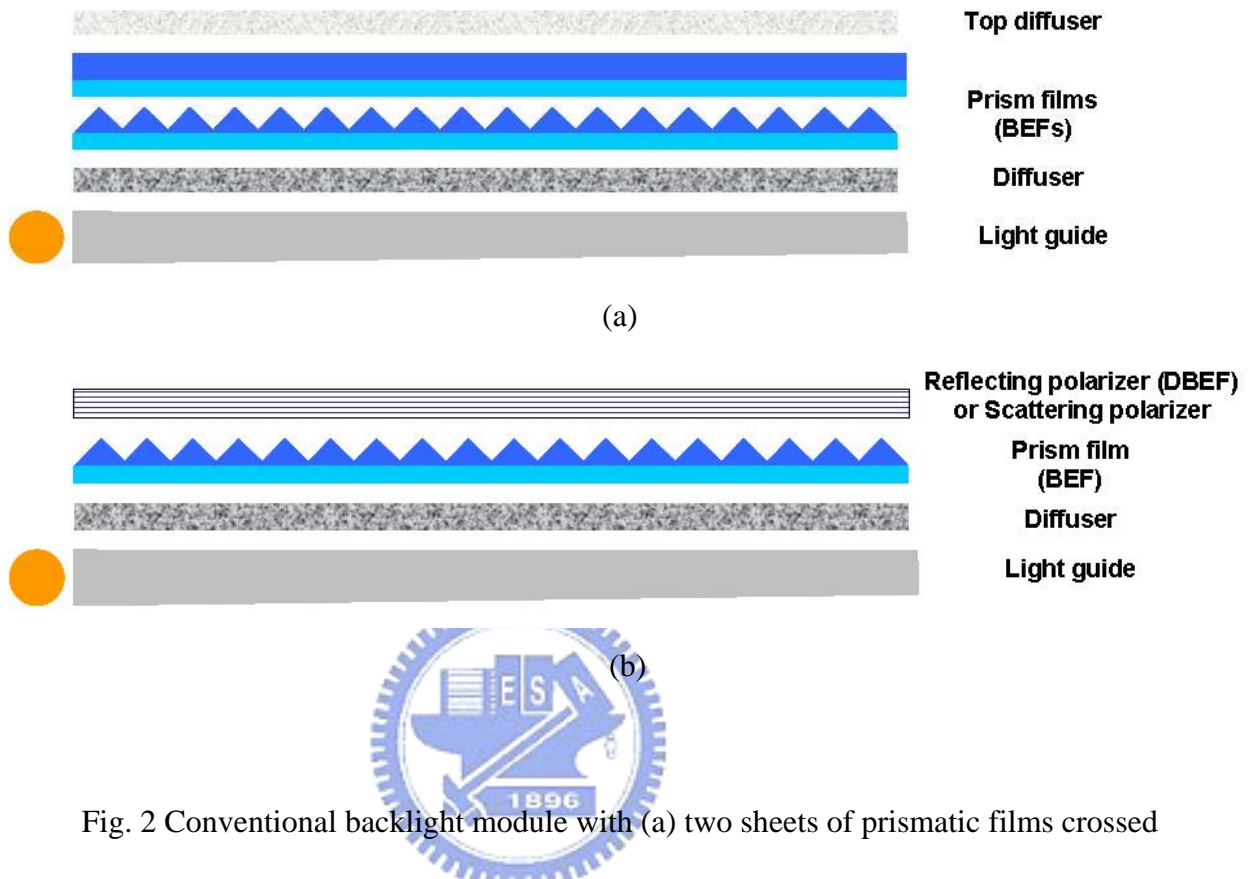


Fig. 2 Conventional backlight module with (a) two sheets of prismatic films crossed at 90° (b) single sheet of prismatic film and reflecting polarizer

1.2.1 Diffuser

The top diffuser in Fig. 2(a) protects the prismatic film from scratching and decreases the Moirè effect caused by the periodic structure of the prismatic films and the liquid crystal cells. Although the micro-structures of the light guide perform a light diffusion function for light uniformity over the whole panel, the light uniformity of the light guide is still not sufficient. A diffuser that scatters light extracting from the light guide and distributes light evenly across the viewing area is used to compensate the light guide for insufficient light uniformity.

1.2.2 Brightness Enhancement Films (BEF)

One or two sheets of orthogonally-crossed BEFs that utilize prismatic surface structures are treated as light-collecting films to redistribute light and enhance the axial luminance along the normal viewing direction [2]. The prism angle of the BEF is fixed at 90° , and the prism pitches is $50\ \mu\text{m}$. The light within the viewing cone whose cone angle is up to $\pm 35^\circ$ off the perpendicular is refracted toward the viewer. Light outside this angle is reflected back and recycled by multiple refraction and total internal reflection, as shown in Fig. 3. On-axis intensity is enhanced up to 153% with one BEF and 225% with two orthogonally-crossed BEFs, as shown in Fig. 4. The dotted line represents the light source with lambertian distribution as the reference, in which the maximum radiant intensity is normalized to be 1. Since the Moirè effect which results from the interference between the periodic structures of BEFs and LC cells is easily perceived by human eyes. The top diffuser above BEFs or micro-structure film with randomized pitches are applied to reduce the Moirè effect [3].

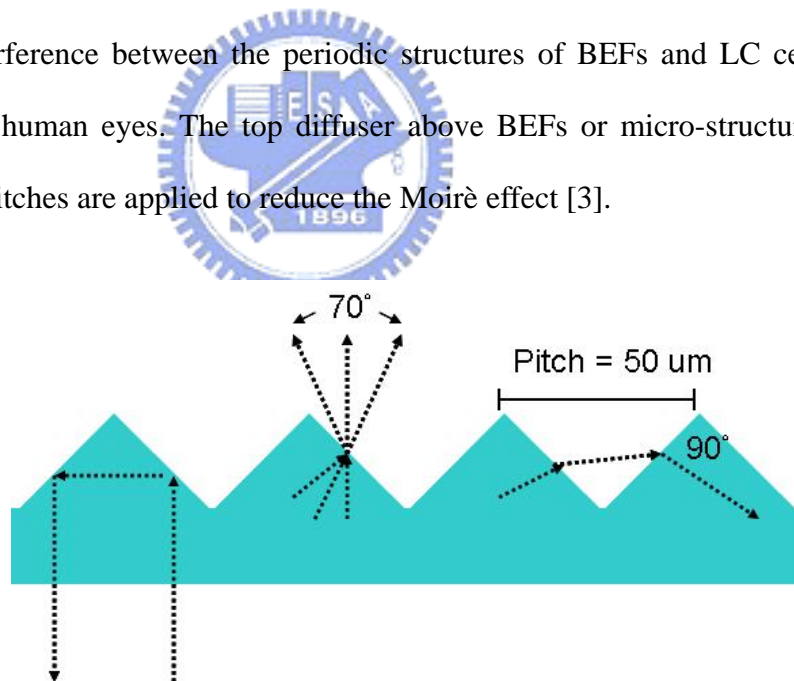


Fig. 3 BEF with pitch of $50\ \mu\text{m}$ and prism angle fixed at 90°

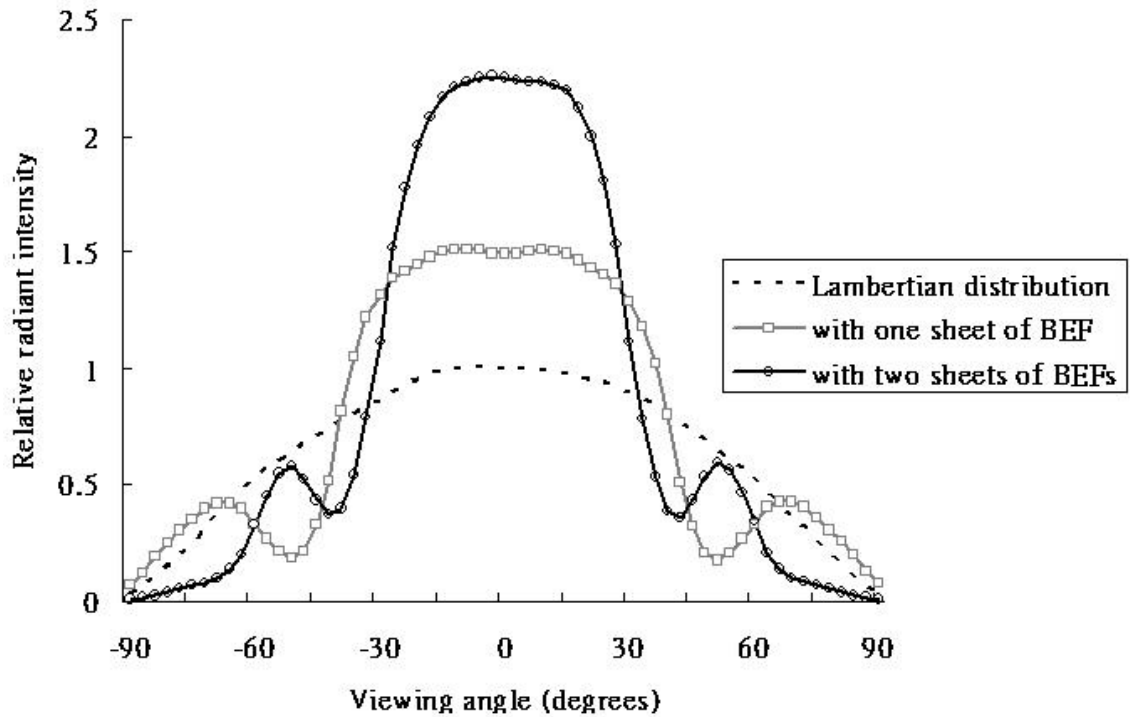


Fig. 4 On-axis intensity enhancement of the BLM with BEFs

1.3 Polarizer

1.3.1 Absorbing Polarizer

The conventional dichroic polarizer based on absorption is a multi-layer sandwich of iodine containing a stretched PVA film between sheets of tri-acetate cellulose (TAC) whose absorption properties are strongly dependent on the direction of the vibration of the electric field, as shown in Fig. 5.

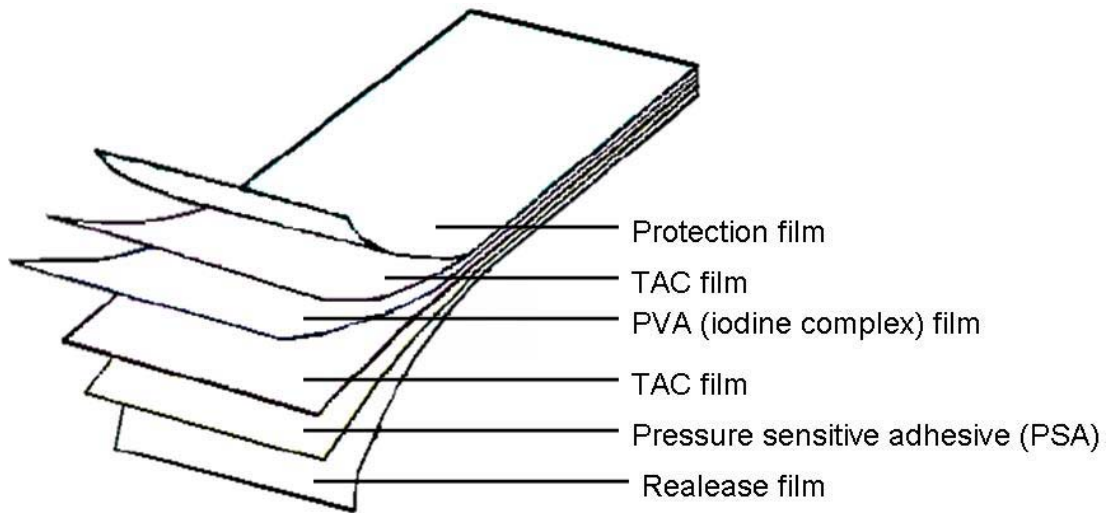


Fig. 5 Dichroic polarizer in LCD Displays

A sheet of PVA is one-dimensionally stretched and dipped into an ink of iodine. Thus the long molecules of PVA are aligned, and the iodine impregnates PVA to form PVA-iodine complex. The mechanism of long-chain molecules are similar to long thin wires. When the E field is parallel to the molecules, a current is induced in the axial direction. Finally the induced current is strongly absorbed by iodine complex and converted into heat. The transmission axis is therefore perpendicular to the direction in which the film was stretched, as shown in Fig. 6.

Natural light that is also known as unpolarized light can be decomposed into two arbitrary and orthogonal waves. A dichroic linear polarizer transmits 50% of the incident natural light and absorbs the other 50%. In fact, however, about 4% of the incident light will be reflected back at each surface of the ideal polarizer (100% of polarization efficiency) without using of antireflection coatings. Finally only about 46% of the incident light can be utilized when the other 54% was absorbed or reflected. With reflective polarizer or scattering polarizer, the light polarized in the direction of the

absorption axis can be recycled instead of being absorbed.

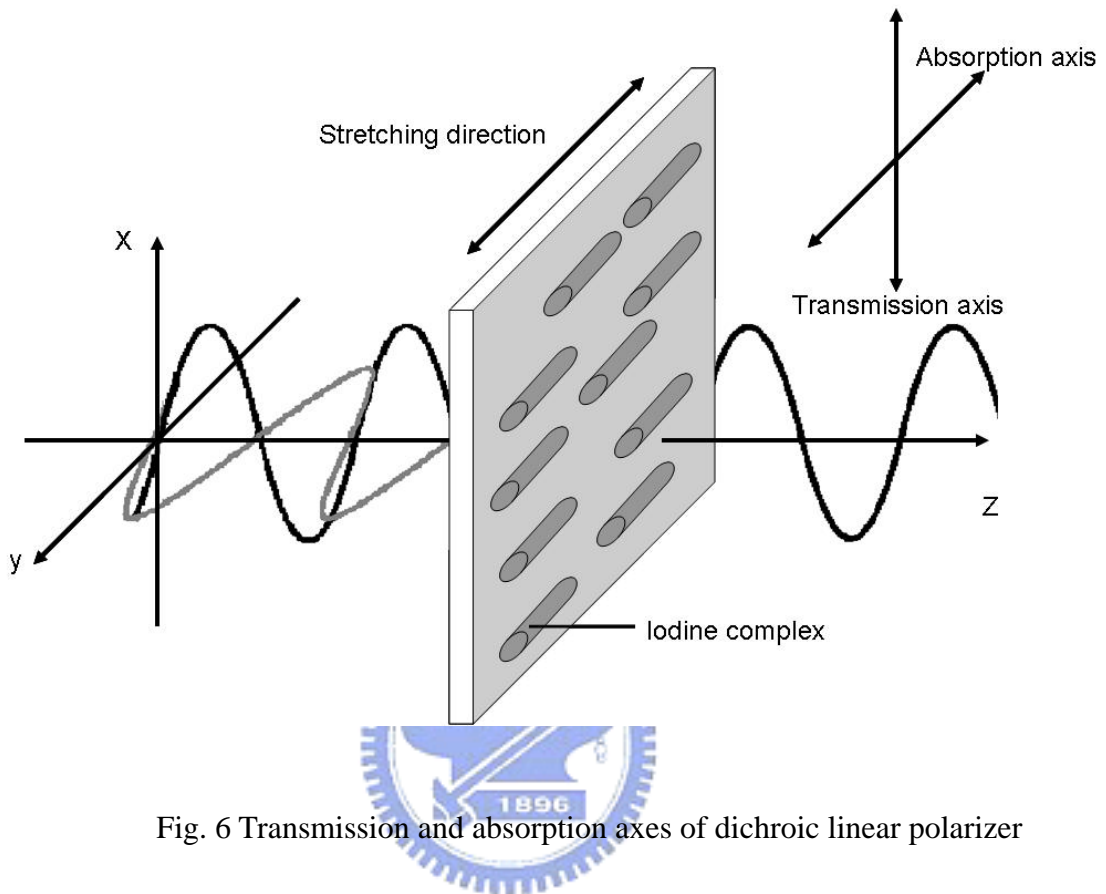


Fig. 6 Transmission and absorption axes of dichroic linear polarizer

1.3.2 Reflecting Polarizer

The dual brightness enhancement film (DBEF) which consists of multilayer laminates is a sort of reflective polarizer and works through polarization recycling [4]. A conventional dichroic polarizer allows only 50% of the light to pass, the s -wave, and absorbs the other 50%, the p -wave. The DBEF is formed by the periodically multilayer with alternating indices of refraction. Each layer in the DBEF contains a isotropic and a birefringent film. The refraction index of the ordinary wave in the birefringent medium is equal to the refraction index of the isotropic film, as shown in Fig. 7. For the linear polarized light whose direction of polarization is in the direction of the ordinary wave, the s -wave, the DBEF is isotropic, and therefore this light can pass through the DBEF.

The complementary beam polarized in the direction of the extraordinary wave, the p -wave, is reflected into the backlight due to the mismatch of the refraction indices if the layer period is matched with the wavelength. The reflected light is reflected again by a depolarizing diffuser in the BLM, hence it can be recycled, as shown in Fig. 8. It is reported that the brightness can increase up to 50% with DBEF applied in the BLM [5].

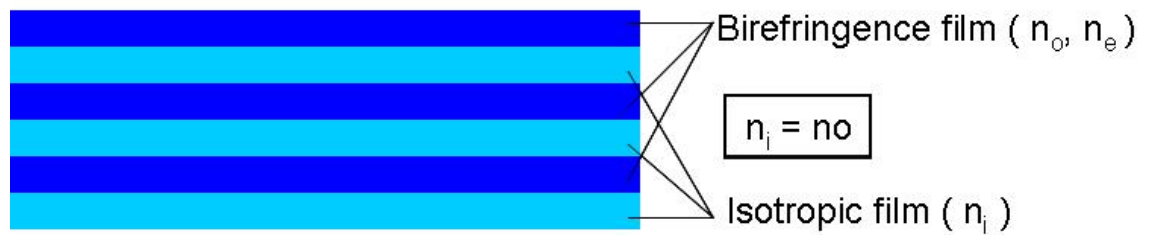


Fig. 7 DBEF with multilayer structures

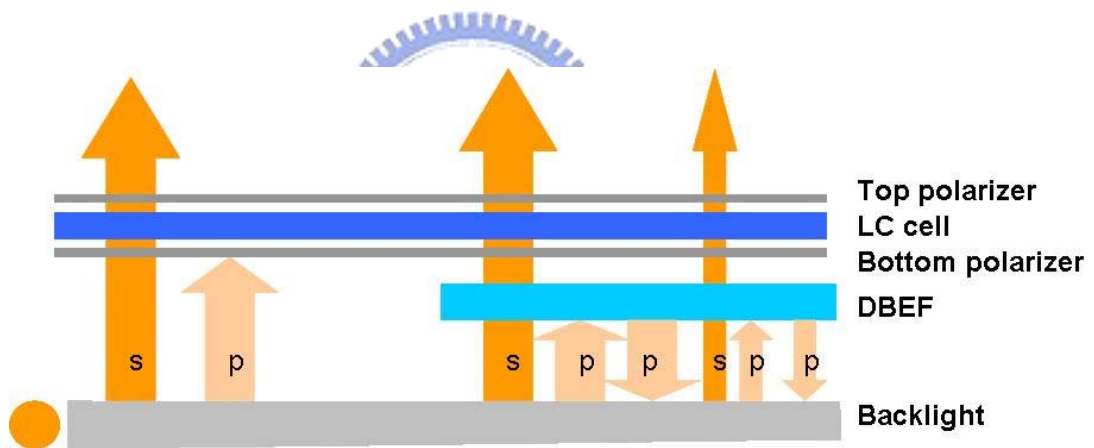


Fig. 8 LCD display enhanced by DBEF

The reflecting polarizer based on a cholesteric film is a birefringent foil with helical molecular structure where the helical axis lies normal to the plane of the film [6]. The cholesteric helix only allows the light circularly polarized in the opposite sense to the helical pitch to pass while the light circularly polarized in the same sense as the helix is reflected, as shown in Fig. 9. The reflected ray can be depolarized and reflected back from a reflector system commonly incorporated into the BLM used in LCDs. Thus the

reflected light is recycled back onto the cholesteric film. Ideally, nearly all the light can be transmitted as circularly polarized light. The circularly polarized light at the output of the cholesteric film is converted to linearly polarized light by a quarter wave plate which can be utilized by the conventional linear polarizer on any LCD. The displays can be as much as 80% brighter with the reflecting polarizer based on a cholesteric film used in the BLM [7]. However, the additional quarter wave plate will increase the thickness of the structure, and the fabrication process is expensive.

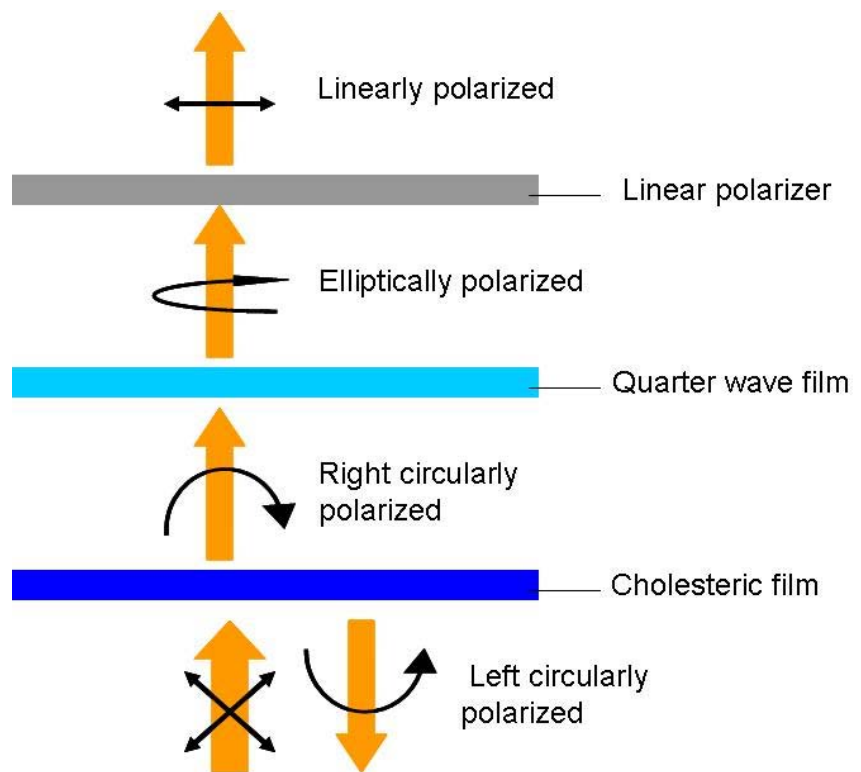


Fig. 9 The mechanism of the reflecting polarizer based on a cholesteric film with a quarter wave plate

1.3.3 Scattering Polarizer

The scattering polarizers, such as one-dimensionally stretched phase separated polymer films, isotropic particle dispersed one-dimensionally stretched polymer films, and one-dimensionally stretched PDLC films, are created by using composite materials.

Among the different methods to create scattering polarizers, the one-dimensionally stretched PDLC films is the focus of this contribution due to the simple structure and less expansive fabrication process. The polarization selectivity of the stretched PDLC films arises from anisotropic scattering of aligned liquid crystal droplets in a polymer matrix, hence backscattered light can be recycled in the BLM to enhance the optical efficiency, as shown in Fig. 10 [8][9]. The mechanism of polarization recycling by utilizing the stretched PDLC films will be further described in Sec. 2.2.2.

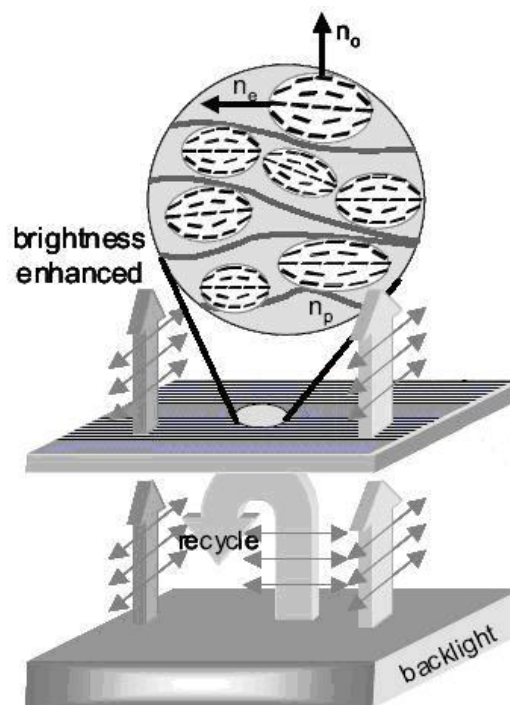


Fig. 10 A scattering polarizer based on PDLC technology

1.4 Motivation and Objective

The conventional dichroic polarizer is a key component in LCD displays. However, only 50% of light are allowed to transmit through the dichroic polarizer. To pursue higher light efficiency, the stretched PDLC film, a sort of scattering polarizer, can be

applied in LCD displays to improve brightness by polarization recycling. Since scattering polarizers can possibly be less expensive to fabricate than reflecting polarizers and have the benefit of recycling light which would have been absorbed in conventional polarizers, these devices can be candidates in LCDs where power saving is one of the highest priorities.

As a result, the objective of this thesis is to fabricate stretched PDLC films and research the optical characteristics of PDLC films. Besides, the azimuthal polarizers which can be used as polarization axis finders are realized by two-dimensional radially stretching of the PDLC films. The properties of azimuthal polarizers will also be described in this thesis.

1.5 Organization of This Thesis

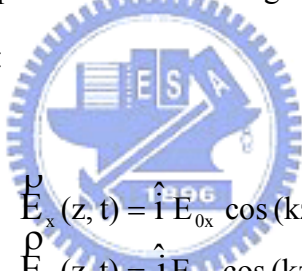
The thesis is organized as following : The principle of the polarization and the mechanism of one-dimensional linearly and two-dimensional radially stretched PDLC films are presented in **Chapter 2**. In **Chapter 3**, the fabrication process of the PDLC films and the measurement instruments are introduced in detail. The discussion of the experimental results and the conclusion of this thesis will be presented in **Chapter 4 and 5**.

Chapter 2

Principle

2.1 Polarization of Optical Waves

Light which can be treated as transverse electromagnetic waves in the electromagnetic theory of light is often represented by its electric field vector [10, 11]. The orientation of the electric field is constant, although its magnitude and sign vary in time and space as the light propagates. A transverse optical wave that propagates along the z axis can be decomposed into two orthogonal components of electric field, which are expressed as below :


$$\begin{aligned} \vec{E}_x(z, t) &= \hat{i} E_{0x} \cos(kz - \omega t) \\ \vec{E}_y(z, t) &= \hat{j} E_{0y} \cos(kz - \omega t + \delta) \end{aligned} \quad (1)$$

where E_{0x} and E_{0y} are two independent amplitudes, and δ is the relative phase difference between the two waves and limited in the region $-\pi < \delta \leq \pi$. The resultant optical wave is the vector sum of these two orthogonal waves :

$$\vec{E}(z, t) = \vec{E}_x(z, t) + \vec{E}_y(z, t) \quad (2)$$

When the two waves are in-phase ($\delta = 0$) or 180° out-of phase ($\delta = \pi$), the resultant wave whose electric field vector oscillates sinusoidally along a constant direction in xy plane is said to be linearly polarized, as shown in Fig. 11.

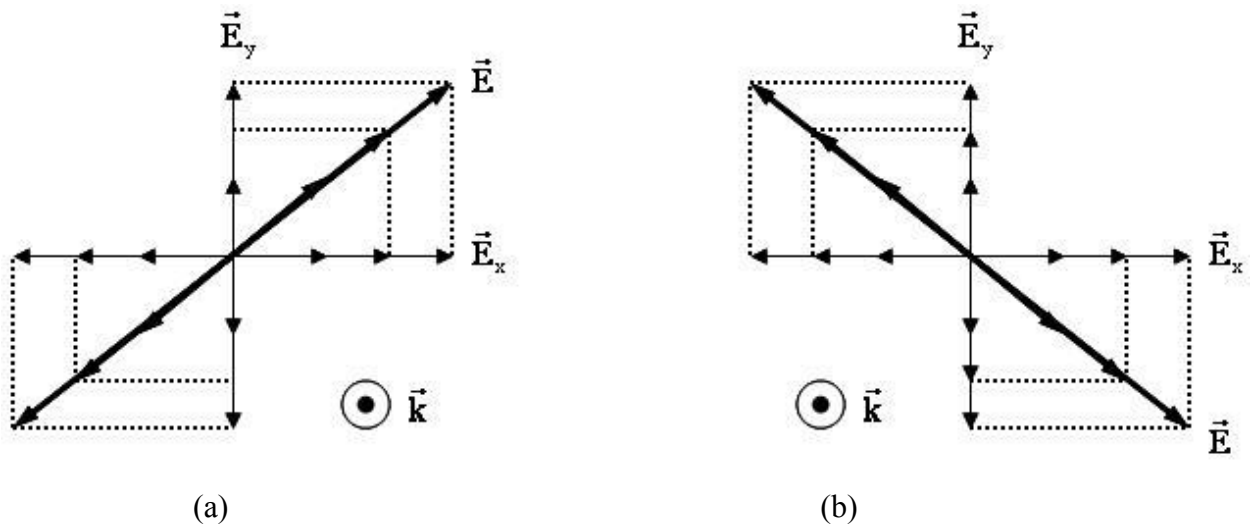


Fig. 11 Light linearly polarized (a) in the first and third quadrants ($\delta = 0$) (b) in the first and third quadrants ($\delta = \pi$) oscillating in time

Another case of importance is the circular polarization, which occurs when $E_{0x} = E_{0y}$ and $\delta = \pm \frac{1}{2} \pi$. Accordingly

$$\begin{aligned} \vec{E}_x(z, t) &= \hat{i} E_0 \cos(kz - \omega t) \\ \vec{E}_y(z, t) &= \hat{j} E_0 \cos(kz - \omega t \pm \frac{1}{2} \pi) = \mu \hat{j} E_0 \sin(kz - \omega t) \end{aligned} \quad (3)$$

The resultant wave is

$$\vec{E}(z, t) = E_0 [\hat{i} \cos(kz - \omega t) \pm \mu \hat{j} \sin(kz - \omega t)] \quad (4)$$

The light is right-hand circularly polarized with $\delta = - \frac{1}{2} \pi$, which undergoes a

clockwise rotation of the electric field vector in the xy plane and left-hand circularly polarized with $\delta = \frac{1}{2}\pi$, which undergoes a counterclockwise rotation of the electric field vector in the xy plane, as seen by an observer looking back at the source. The circularly polarized light is depicted in Fig. 12.

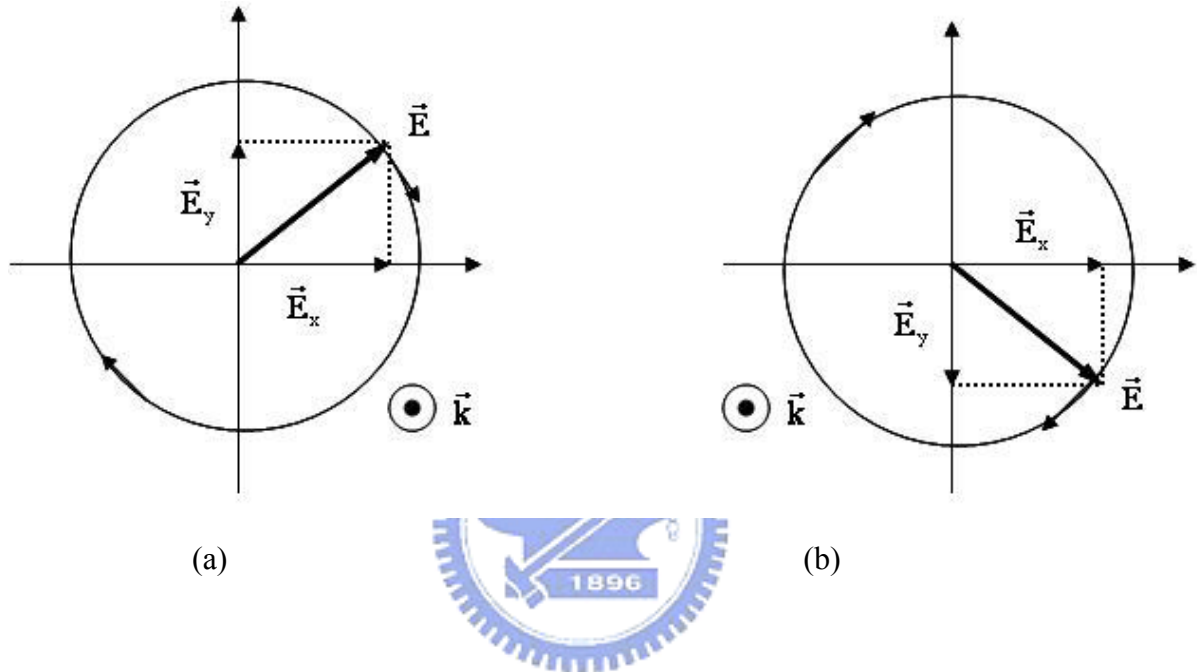


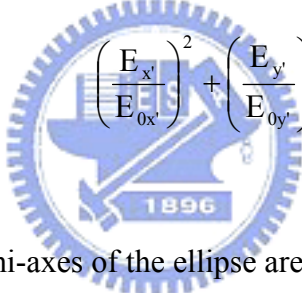
Fig. 12 (a) Right-hand circularly polarized light with the electric field rotating clockwise (b) left-hand circularly polarized light with the electric field rotating counterclockwise

The elliptical polarization is the most general case of a polarized light. Both linear polarization and circular polarization are considered to be special cases of elliptical polarization. The equation of the ellipse making an angle θ with the xy coordinate can be obtained by several steps of elementary algebra of combining the two equations in Eq. (1).

$$\left(\frac{E_x}{E_{0x}}\right)^2 + \left(\frac{E_y}{E_{0y}}\right)^2 - 2\left(\frac{E_x}{E_{0x}}\right)\left(\frac{E_y}{E_{0y}}\right)\cos\delta = \sin^2\delta \quad (5)$$

$$\tan 2\theta = \frac{2E_{0x}E_{0y}\cos\delta}{E_{0x}^2 - E_{0y}^2} \quad (6)$$

Eq. (5) can be diagonalized by a transformation of the coordinate system. The new axes of the new coordinate system, x' and y' , are along the principal axes of the ellipse, as shown in Fig. 13. Thus the new equation of the ellipse in the $x'y'$ coordinate becomes



$$\left(\frac{E_{x'}}{E_{0x'}}\right)^2 + \left(\frac{E_{y'}}{E_{0y'}}\right)^2 = 1 \quad (7)$$

The length of the principal semi-axes of the ellipse are given by

$$\begin{aligned} E_{0x'}^2 &= E_{0x}^2 \cos^2\theta + E_{0y}^2 \sin^2\theta + 2E_{0x}E_{0y}\cos\delta \cos\theta \sin\theta \\ E_{0y'}^2 &= E_{0x}^2 \sin^2\theta + E_{0y}^2 \cos^2\theta - 2E_{0x}E_{0y}\cos\delta \cos\theta \sin\theta \end{aligned} \quad (8)$$

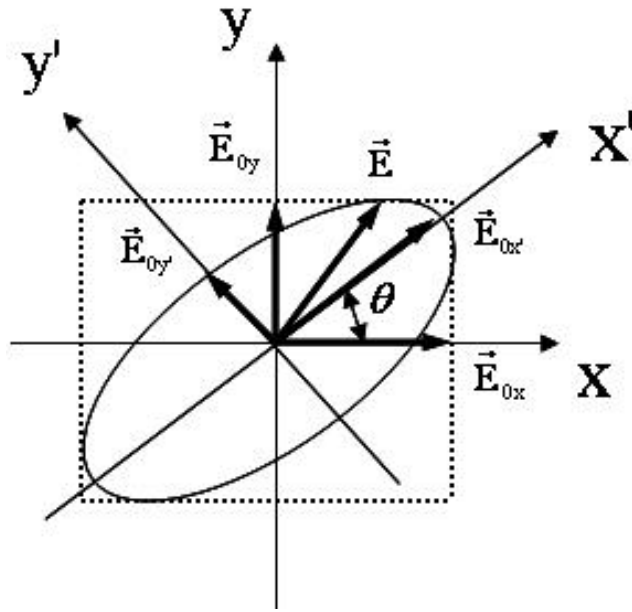


Fig. 13 Elliptically polarized light

The light is right-hand elliptically polarized with $\sin\delta < 0$ and left-hand elliptically polarized with $\sin\delta > 0$, as shown in Fig. 14. The comparison of the linear and circular polarization which is the special case of the elliptical polarization is listed in Table 1.

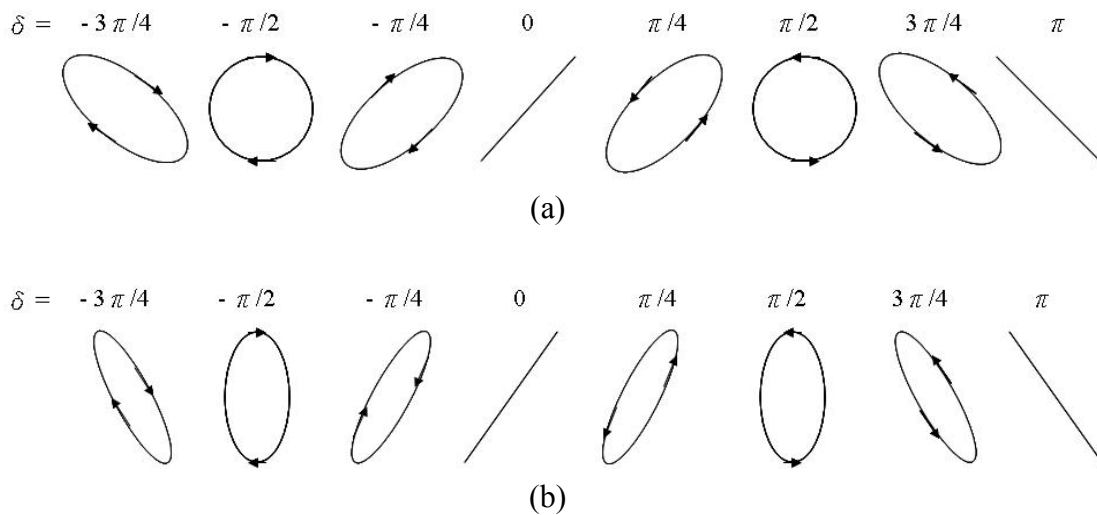
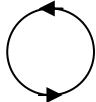
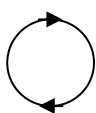


Fig. 14 Elliptical polarization configuration at various relative phase difference δ when (a) $E_{0y} = E_{0x}$ and (b) $E_{0y} > E_{0x}$

Tab. 1 Comparison of state of polarization

	δ	Direction	Amplitude	
Linear Polarization	$\delta = 0, \pi$	 $\delta = 0$		Special Case of Elliptical Polarization
		 $\delta = \pi$		
Circular Polarization	$\delta = \pm \frac{1}{2} \pi$	 $\delta = \frac{1}{2} \pi$ Left-hand	$E_{0x} = E_{0y}$	
		 $\delta = -\frac{1}{2} \pi$ Right-hand		
Elliptical Polarization	$0 < \delta \leq \pi$	 $\sin \delta > 0$ Left-hand		
		 $\sin \delta < 0$ Right-hand		

2.2 Spatially Inhomogeneous Polarized Beam

The spatially homogeneous polarized beam is defined as the beam with the same polarization at all points in the pupil plane, i.e. $\vec{E}(x, y) = E_x \hat{i} + E_y \hat{j}$. The homogeneous polarized beam with linear polarization (in x-direction), right-hand circular polarization and left-hand polarization are depicted in Fig. 15(a).

In addition, the spatially inhomogeneous polarized beam has specific state of polarization at every local point in the pupil plane, as shown in Fig. 15(b). The local electric field can be defined as $\vec{E}_i(x_i, y_i) = E_{x,i} \hat{i} + E_{y,i} \hat{j}$ where i is the positional index of a local point. The total field can be presented by the summation of each local state of polarization :

$$\vec{E}_{\text{total}}(x, y) = \sum_{i=1}^n \vec{E}_i(x_i, y_i) \quad (9)$$

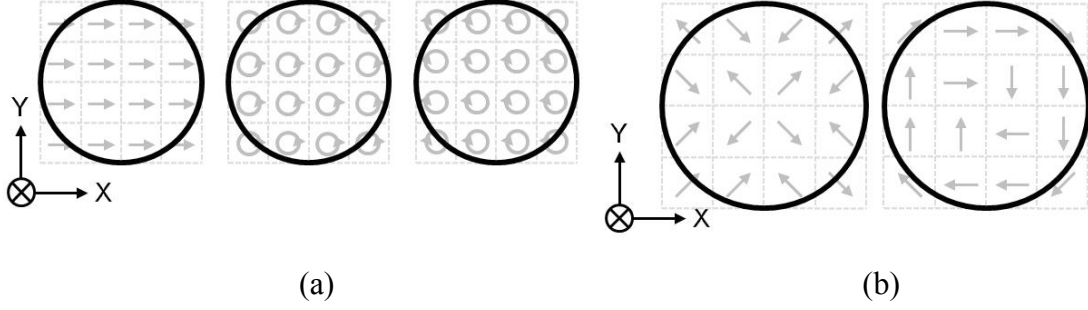


Fig. 15 (a) The spatially homogeneous polarized beam and (b) the spatially inhomogeneous polarized beam

2.2.1 Cylindrical Vector Beam

The cylindrical vector beam which has symmetric distribution on polarization is the special case of the spatially inhomogeneous polarized beams [12]. The cylindrical vector beam has been researched in recent years due to its unique properties resulted from the state of polarization. The general solutions of the wave equation for the cylindrical vector beam are two independent ones which are azimuthally polarized beam and radially polarized beam. The azimuthally and radially polarized beams have cylindrical symmetry in field-amplitude and polarization. The two normal cylindrical vector beams have donut-like field distribution and are symmetric in r -direction and ϕ -direction, as shown in Fig. 16. The field of azimuthally and radially polarized beams can be presented by $\vec{E}_{\text{ap}}(r, \phi) = E_0(\phi)\hat{\phi}$ and $\vec{E}_{\text{rp}}(r, \phi) = E_0(r)\hat{r}$ respectively.



Fig. 16 The field distribution of the cylindrical vector beams (a) radially polarized beam and (b) azimuthally polarized beam where the arrows represent the polarization directions

2.3 Polymer dispersed Liquid Crystal (PDLC)

2.3.1 PDLC Light Modulator [13]

A polymer dispersed liquid crystal film is a homogeneous mixture of polymer and micro-sized nematic liquid crystal droplets, as shown in Fig. 17. The liquid crystal material of the microdroplets is positive birefringent ($n_e > n_o$), and the refraction index n_p of the polymer is chosen to be close to the ordinary refraction index n_o of the liquid crystal.

$$\begin{aligned} n_o &= n_p \\ n_e &> n_p \end{aligned} \quad (10)$$

In the undriven state, the orientation of the nematic liquid crystal in the microdroplets is arbitrary with respect to the plane of the film, and the difference between the refraction index of the polymer and the effective refraction index of the liquid crystal results in scattering of the incident light. The film appears opaque for the severe scattering of light. When the external electric field is applied to the film, the liquid crystal in the droplets is aligned, and the director is parallel to the field because of the

positive birefringence. Since the ordinary refraction index of the liquid crystal is matched to the refraction index of the polymer, the incident light with a normal incident angle encounters no variation in refraction index and transmits through the film without being scattered. Thus it's possible to control the intensity of transmitted light by changing the orientation of the liquid crystal molecules with an electric field.

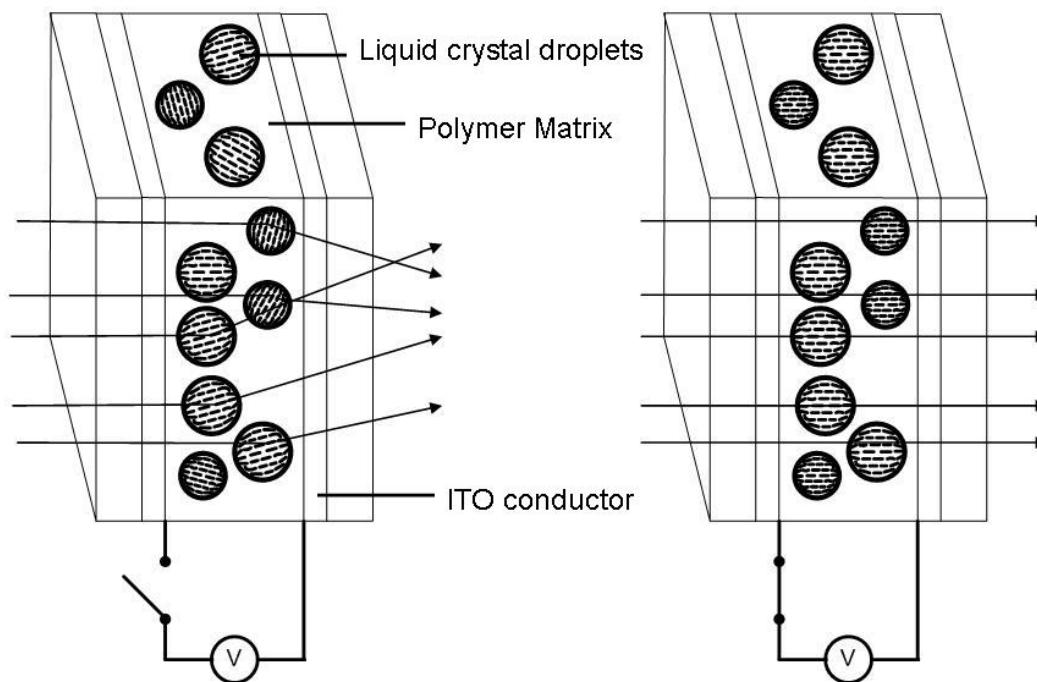


Fig. 17 Polymer dispersed liquid crystal (PDLC) light modulator

For angles of the incident light other than normal, the liquid crystal droplets are optically birefringent. One polarization component will see the ordinary refraction index n_o , while the other polarization component will see the effective refraction index $n_e(\theta)$ as below :

$$\frac{1}{n_e^2(\theta)} = \frac{\sin^2 \theta}{n_e^2} + \frac{\cos^2 \theta}{n_o^2} \quad (11)$$

where θ is the angle between the optical axis and the direction of propagation in the droplets. The difference between n_p and $n_e(\theta)$ results in a small amount of scattering at the boundary of the droplets, increasing with angle θ , as shown in Fig. 18. The films appear hazy because of the decrease in the transmission when viewed at large viewing angles.



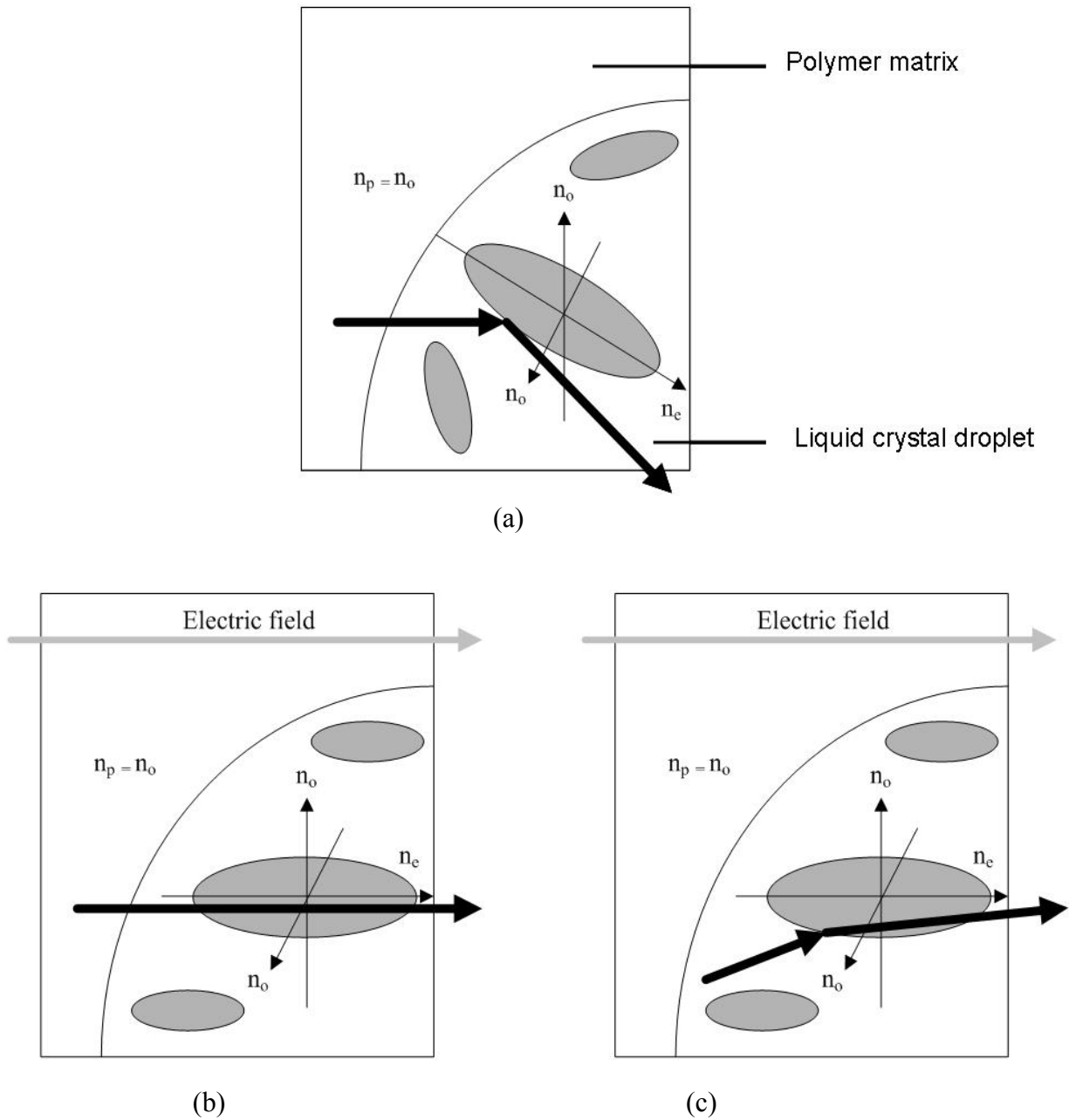


Fig. 18 The scattering mechanism of the PDLC operation. (a) Off-state
 (b) On state – viewing at the normal (c) On state – viewing off-axis

2.3.2 Elongation of Liquid Crystal Droplets

In PDLC films, the liquid crystal droplets are non-spherical and can be

approximated by an ellipse with a small aspect ratio. The strain arising from the matrix polymerization process during solvent evaporation results in the distortion of droplet shape. The liquid crystal molecules in the droplets can be aligned in different director fields depending mainly on the interface-anchoring and elastic properties. Thus the bipolar tangential alignment illustrated in Fig. 20(a) is usually observed where the director fields develop along the major axes of the ellipsoidal cavities.

With one-dimensional elongation of liquid crystal droplets, the liquid crystal molecule in the droplets will be also be aligned in the long axis of the prolate droplet. Therefore, the scattering behavior of the PDLC films can be partly controlled. There are three ways to obtain elongated liquid crystal droplets, as shown in Fig. 19 [14]. In the first way, the PDLC film is stretched above the plastic deformation and therefore liquid crystal droplets are deformed and elongated along the stretching direction. The second way is to apply high electric field (about 10-15 V/ μm) on the PDLC film during polymerization. The electric contribution to the liquid crystal elastic deformation free energy enforces droplets elongation. In the third method, curable polymer is utilized. Shearing force is adopted during curing the polymer. Among these three methods, the stretching of the PDLC film is considered to be the simplest and most effective process and adopted in this research.

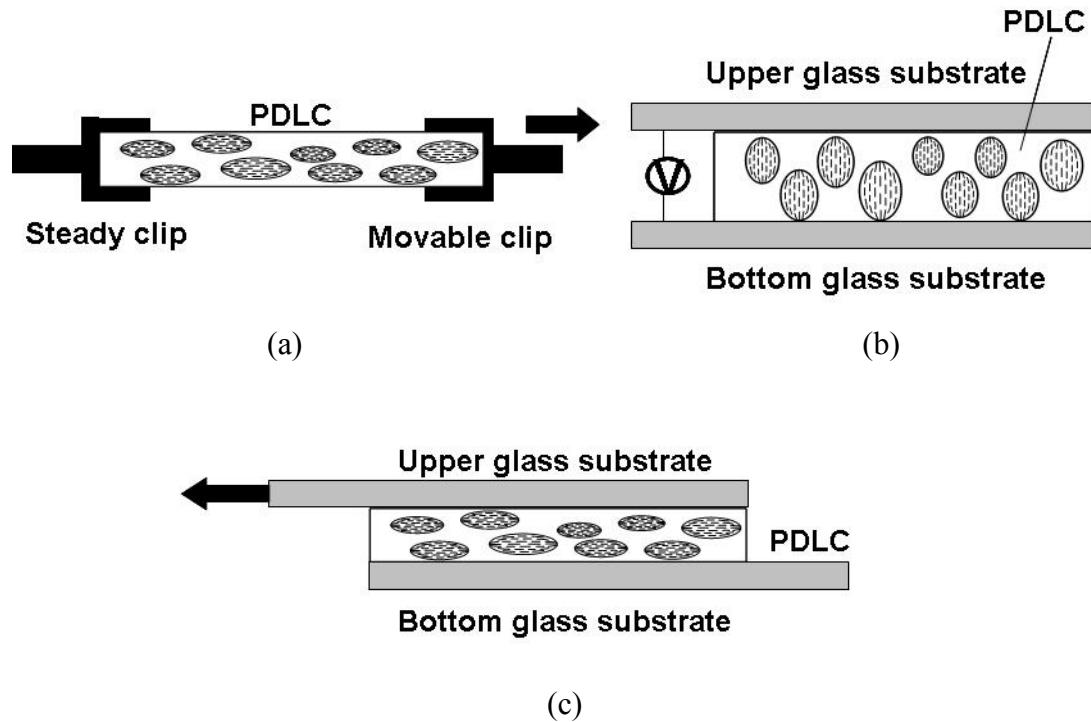


Fig. 19 Technique of elongating liquid crystal droplets (a) Stretching of PDLC film (b) deforming effect of electric field (c) shearing of system

2.3.3 One-dimensional Linearly Stretched PDLC Film

When the one-dimensional strain is applied on the PDLC film, the droplet is elongated along the stretching direction, and the bipolar axes in the cavities are also aligned along this direction due to the anchoring effect of the interface, as shown in Fig. 20(b). A refraction index difference between the axes parallel and perpendicular arises from the parallel alignment of the fields to the stretching direction, as shown in Fig. 21. Since the refraction index of the polymer matrix is almost isotropic, a large refraction index mismatch exists in the direction parallel to the stretching direction while the ordinary refraction index of the liquid crystal n_o is close to the refraction index of the polymer n_p in the direction perpendicular to the stretching direction.

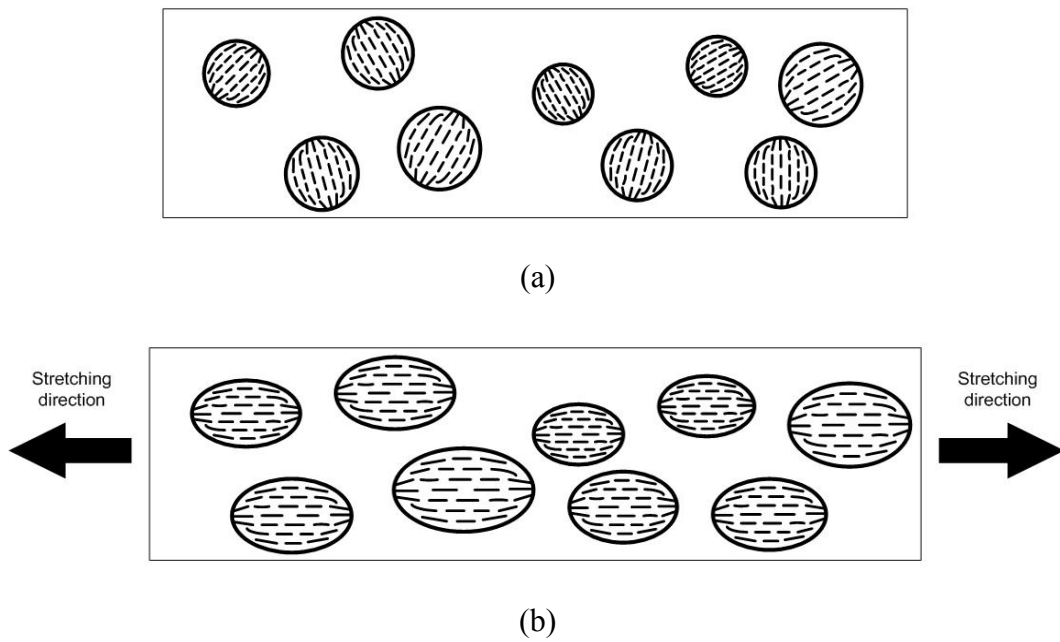


Fig. 20 PDLC films (a) before and (b) after stretching

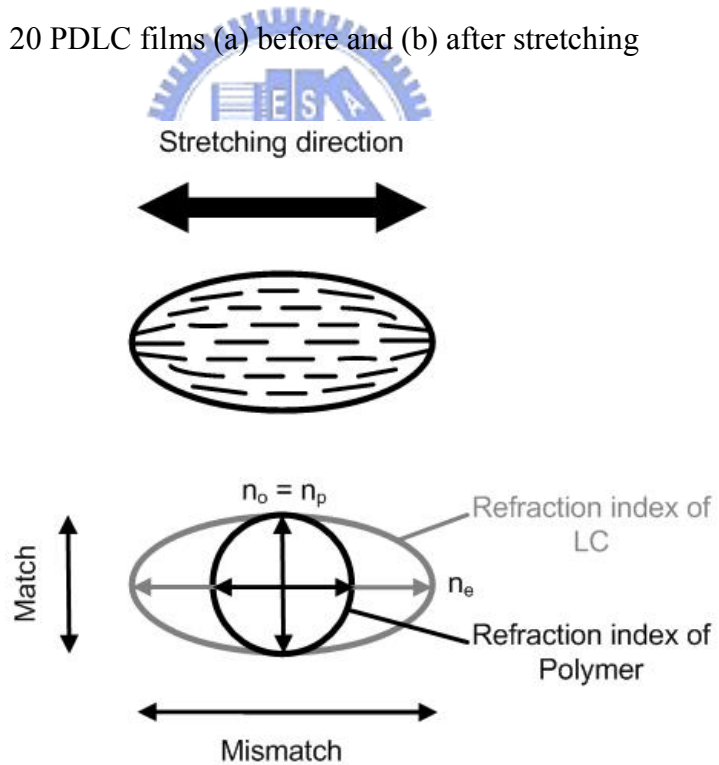


Fig. 21 The refractive index difference in the stretched PDLC films

The one-dimensionally stretched PDLC films can be employed as scattering polarizers due to the polarization selectivity resulting from the unidirectional

alignment of the LC droplets and the parallel alignment of the LC director fields [15]. The linear polarized light whose direction of polarization is perpendicular to the stretching direction can transmit for the refraction index match of n_p and n_o , while the light polarized in the direction of the droplet ordering is strongly scattered due to the mismatch between n_p and n_e , as shown in Fig. 22. Thus the stretched PDLC films as scattering polarizers can enhance light efficiency through polarization recycling.

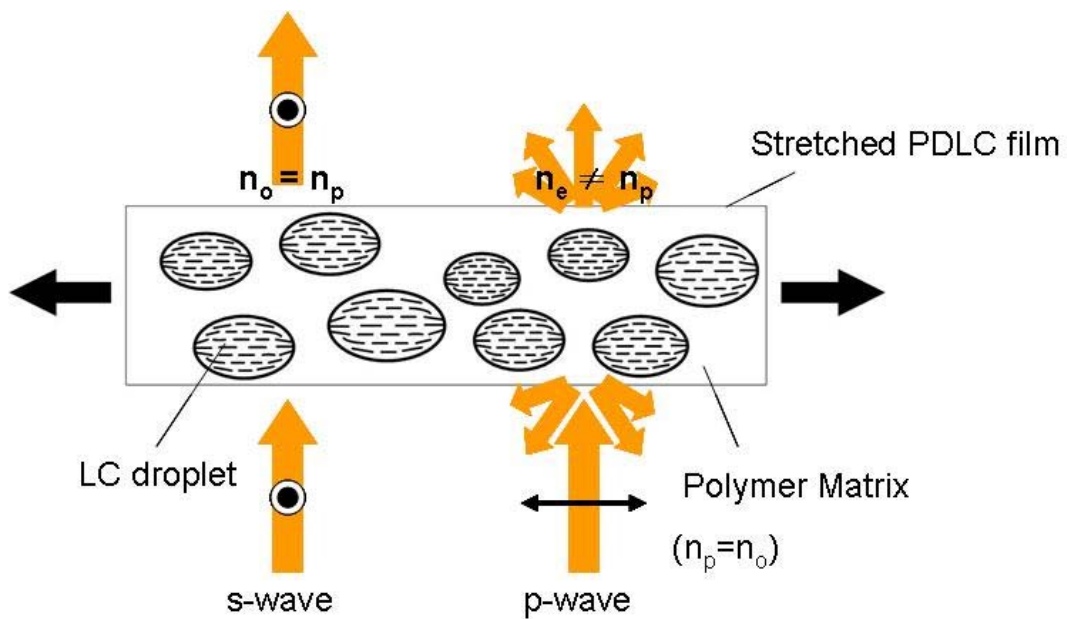


Fig. 22 Mechanism of a scattering polarizer based on PDLC technology

2.3.4 Two-dimensional Radially Stretched PDLC Film

Since the transmission axis of the stretched PDLC films is normal to the stretching direction, special polarizers can be obtained by applying strain in different directions on the PDLC films. The azimuthal polarizer which can be used as a polarization axis finder is fabricated by radially stretching of the film. Thus the transmission axis is along the azimuthal direction, and the unpolarized light can be converted into the state of azimuthal polarization, as shown in Fig. 23.

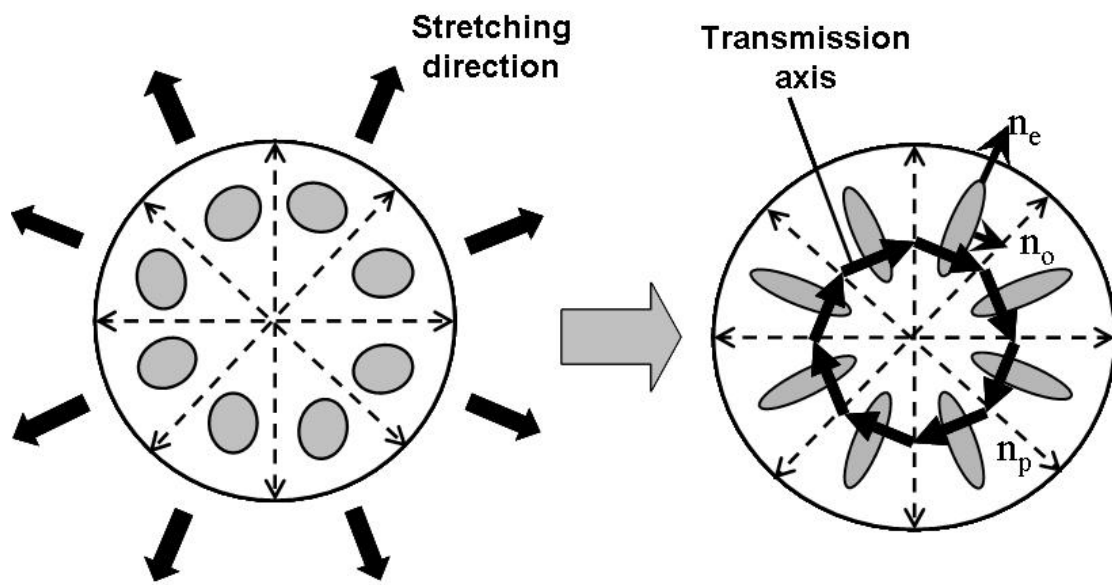


Fig. 23 Mechanism of an azimuthal polarizer by radially stretching of PDLC film



Chapter 3

Fabrication and Measurement Instruments

3.1 Preparation of Stretched PDLC Films

3.1.1 Fabrication of PDLC Films

PDLC films were prepared by encapsulation method in this research[16]. The system was heterogeneous during the whole fabrication process. Liquid crystal was dispersed in a polymer solution , the solvent of which did not dissolve liquid crystal. Polyvinyl-alcohol (PVA) was chosen as the PDLC binder. The solvent evaporation stabilized the obtained composite structure due to polymer solidification.

The detailed steps of fabrication are listed below, and the preparation of the PDLC films is shown schematically in Fig. 24.

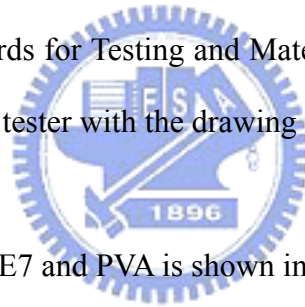
(a) PDLC solution preparation:

- (1) PVA, a water-soluble polymer, was used as the solvent. The nematic liquid crystal E7 (Merck Display Technology, Ltd.) was mixed with a 20 wt% aqueous solution of PVA (PVA 81381, molecular weight 31000, Fluka Analytical) , and the liquid crystal concentration in the PDLC films (PVA with E7) was set 20-45 wt %.
- (2) The solution was then emulsified by agitators, and the bubbles in the solution were driven out by soaking the beaker containing the solution into a ultrasonic

tank.

(b) Film process:

- (1) The emulsion was coated on a polyethylene terephthalate (PET) substrate using a Meyer Bar (coating rod) driven by hands.
- (2) The thin film was dried in the sweatbox to have the water evaporated from the film surface.
- (3) The dried PDLC films were peeled from the PET substrate. The film thickness was 8 to 24 μm depending on the wire size of the Meyer Bar.
- (4) The samples were cut into the H-shape according to the ASTM Standard D 1708 (American Standards for Testing and Materials) and one-dimensionally stretched by a micro-tensile tester with the drawing rate of 0.5 mm/min.

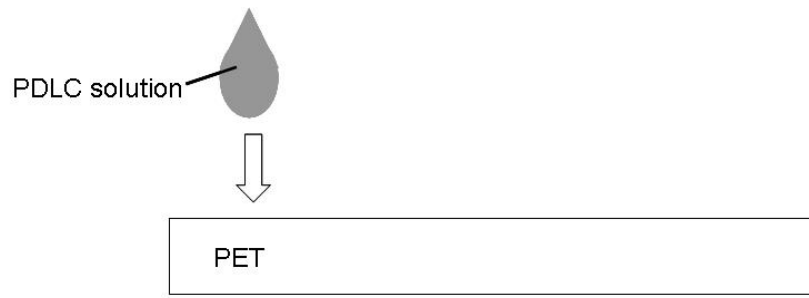


The refraction indices of E7 and PVA is shown in Table 2.

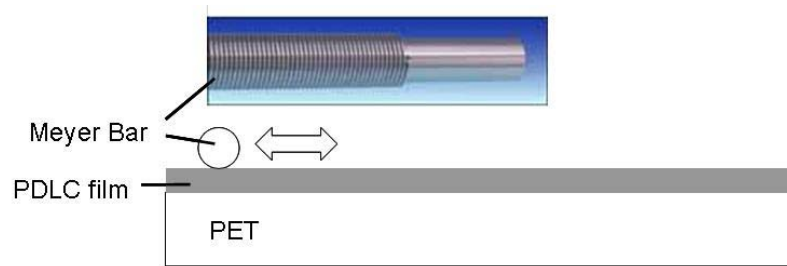
Tab. 2 Refraction indices of E7 and PVA

		Ordinary refraction index n_o	Extraordinary refraction index n_e	Refraction index difference Δn
Liquid Crystal	E7	1.520	1.745	0.225

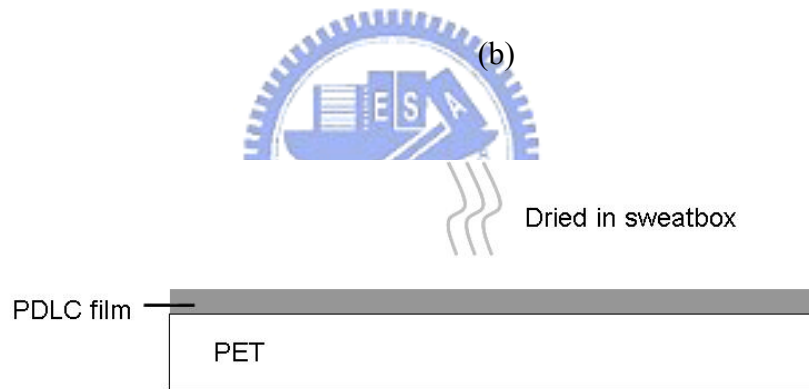
		Refraction index n_p
Polymer	PVA	1.5



(a)



(b)



(c)



(d)

Fig. 24 Flow of preparation of PDLC films (a) the emulsion applied on the PET substrate (b) Meyer Bar coating (c) the film dried in sweatbox (d) the film one-dimensionally stretched by micro-tensile tester

3.1.2 Real-time Measurement Set-up of Optical Properties

The measurement of optical transmittance under different strain as defined in Eq. (12) can be achieved by a real-time measurement set-up as shown in Fig. 25 and 26. The unstretched PDLC film were cut in the shape defined by the American Society for Testing and Materials (ASTM) Standard D 1708, as shown in Fig. 27. The sample was connected to a stress sensor, with a Helium-Neon (He-Ne) laser operating at 633 nm as the light source directed at normal incidence on it. A rotating polarizer was set between the laser and the sample, and polarizations parallel and perpendicular to the stretching direction were investigated. The sample was then one-dimensionally stretched by the micro-tensile tester with the draw rate of 0.5 mm/min. The intensity of the transmitted light was detected by a photodetector while the sample is simultaneously stretched.

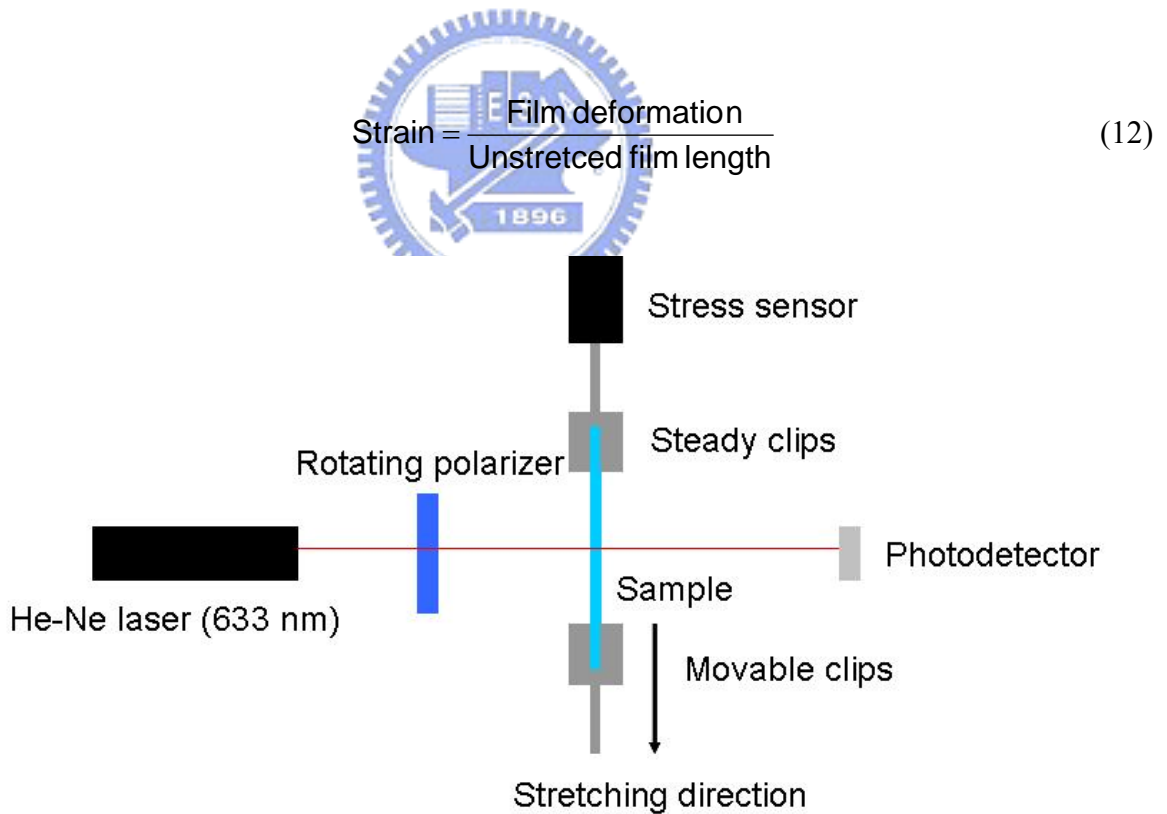


Fig. 25 Schematic representation of real-time measurement set-up

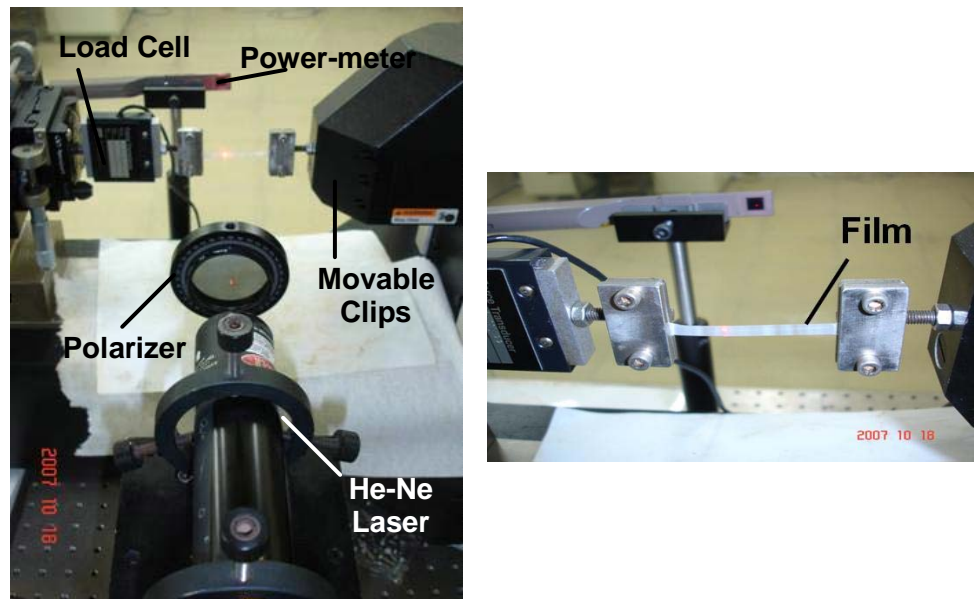


Fig. 26 The pictures of real-time measurement set-up

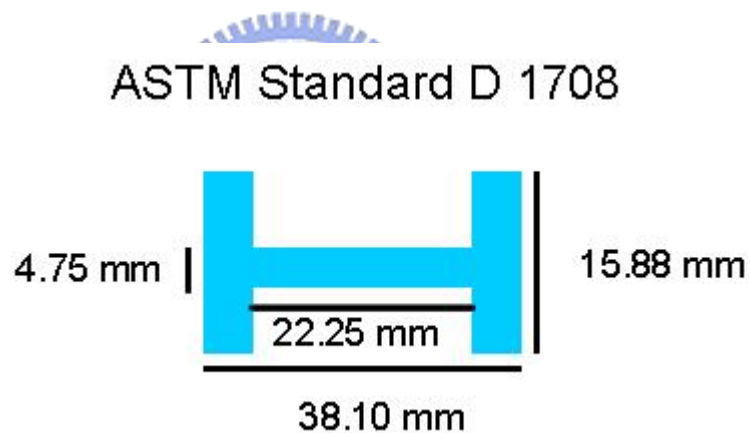


Fig. 27 Samples cut in the shape defined by ASTM standard D 1708

3.1.3 Radially Stretching Process

In the former section, the PDLC films were one-dimensional linearly stretched to obtain linear polarizer. Polarizers with specific polarization function can be achieved by varying the stretching direction. Here the azimuthal polarizer was obtained by radially stretching of the PDLC film.

The steps of fabrication are listed below, and the set-up of radially stretching is shown in Fig. 28.

- (1) The PDLC films whose concentration of E7 is 25 wt% was cut into ‘donut’ shape with radius of 16 mm and attached to the film holder. An o-ring was used at the center of the sample to prevent the sample from breaking.
- (2) A screw across the central hole of the sample was attached to the micro-tensile tester.
- (3) The samples were radially stretched by applying strain at the center of the samples, and the drawing rate of the micro-tensile tester was 0.5 mm/min.

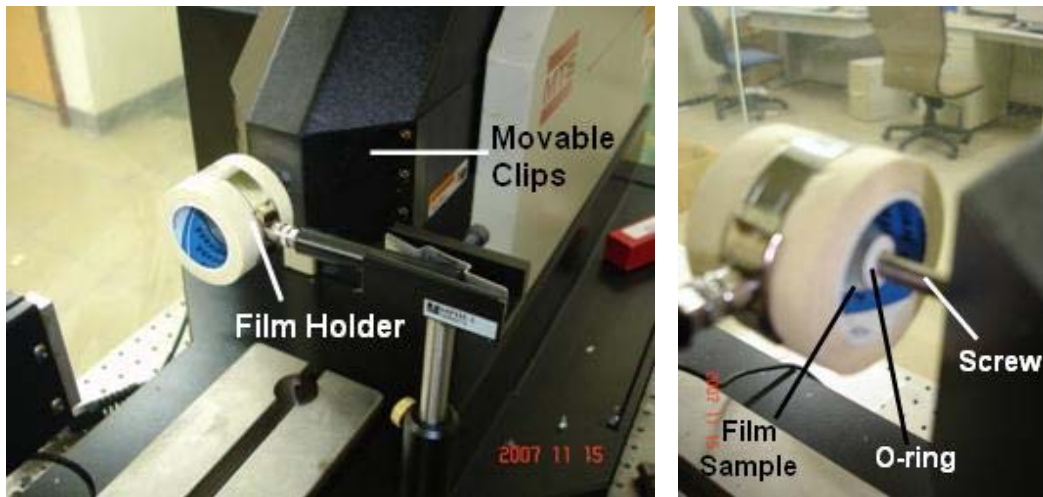


Fig. 28 The set-up of radially stretching process

3.2 FT-IR Spectrometer

A Fourier transform infrared spectrometer (FT-IR) (Nicolet 380, Thermo Electron) with a rotating polarizer, as shown in Fig. 29, is used to investigate the macroscopic orientation of the liquid crystal directors.

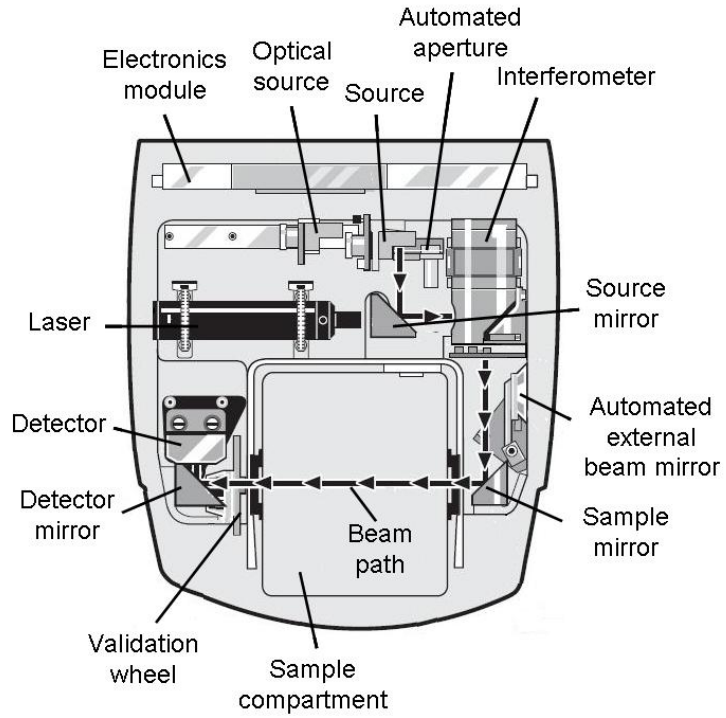


Fig. 29 Inside layout of the FT-IR Spectrometer

The $C\equiv N$ band is representative functional group in E7. When the light is polarized in the direction parallel to the optical axes of E7, a specific wave band at wavenumber 2230 cm^{-1} will be absorbed by the $C\equiv N$ band. The orientation of E7 can be represented by the ordering parameter S defined by Eq. (13)

$$S = \frac{3 \langle \cos^2 \theta \rangle - 1}{2} \quad (13)$$

where θ is the angle between the optical axes of E7 and the stretching direction. S is converted into Eq. (14) by infrared dichroism technique [17].

$$S = \frac{A_{\parallel}/A_{\perp} - 1}{A_{\parallel}/A_{\perp} + 2} \quad (14)$$

where A_{\parallel} and A_{\perp} are the absorbances of the $C\equiv N$ band of E7 at 2230 cm^{-1} , with the infrared beam polarized parallel and perpendicular to the stretching direction of the film. A sample of the IR dichroism in Fig. 30 is indicative of a macroscopic orientation of E7 aligned in the stretching direction where A_{\parallel} is greater than A_{\perp} .

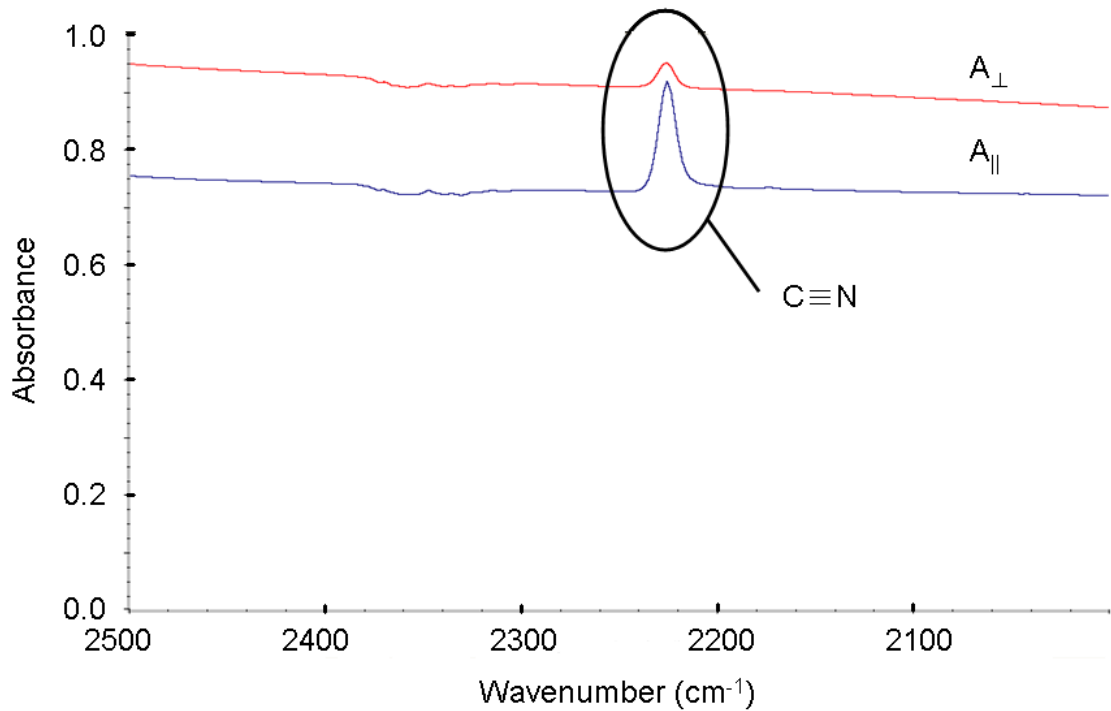


Fig. 30 Polarized infrared spectra of a stretched PDLC film (PVA/E7) with the polarizations of the incident beam parallel and perpendicular to the stretching direction

Chapter 4

Experimental Results and Discussion

4.1 Introduction

The scattering polarizers with polarization recycling can be employed in liquid crystal displays instead of the conventional absorbing polarizers to improve the optical efficiency as mentioned before. Because the scattering polarizers are relatively simple in fabrication process, which can be a potential candidate in portable LCDs where power saving is one of the key issues. Stretching of the PDLC films is one of the most effective way to fabricate scattering polarizers. Besides, the azimuthal polarizer which converts the unpolarized light into azimuthal polarization can be achieved by two-dimensional radially stretching of the PDLC films instead of one-dimensional linearly stretching. A study of the optical properties under different strain will be investigated in this chapter, and the experimental results will be discussed.

4.2 Optical Properties of Stretched PDLC Films

4.2.1 Elongated LC Droplets in Stretched PDLC Films

The PDLC films were stretched under different strain where the liquid crystal droplets were elongated and attained different range of deformation as shown in Fig. 31 and Table 3. The liquid crystal droplets were on the order of several microns as indicated in the optical microscope image. As the films were stretched longer, the aspect ratios of the liquid crystal droplets increased, and the droplets were aligned along the stretching direction.

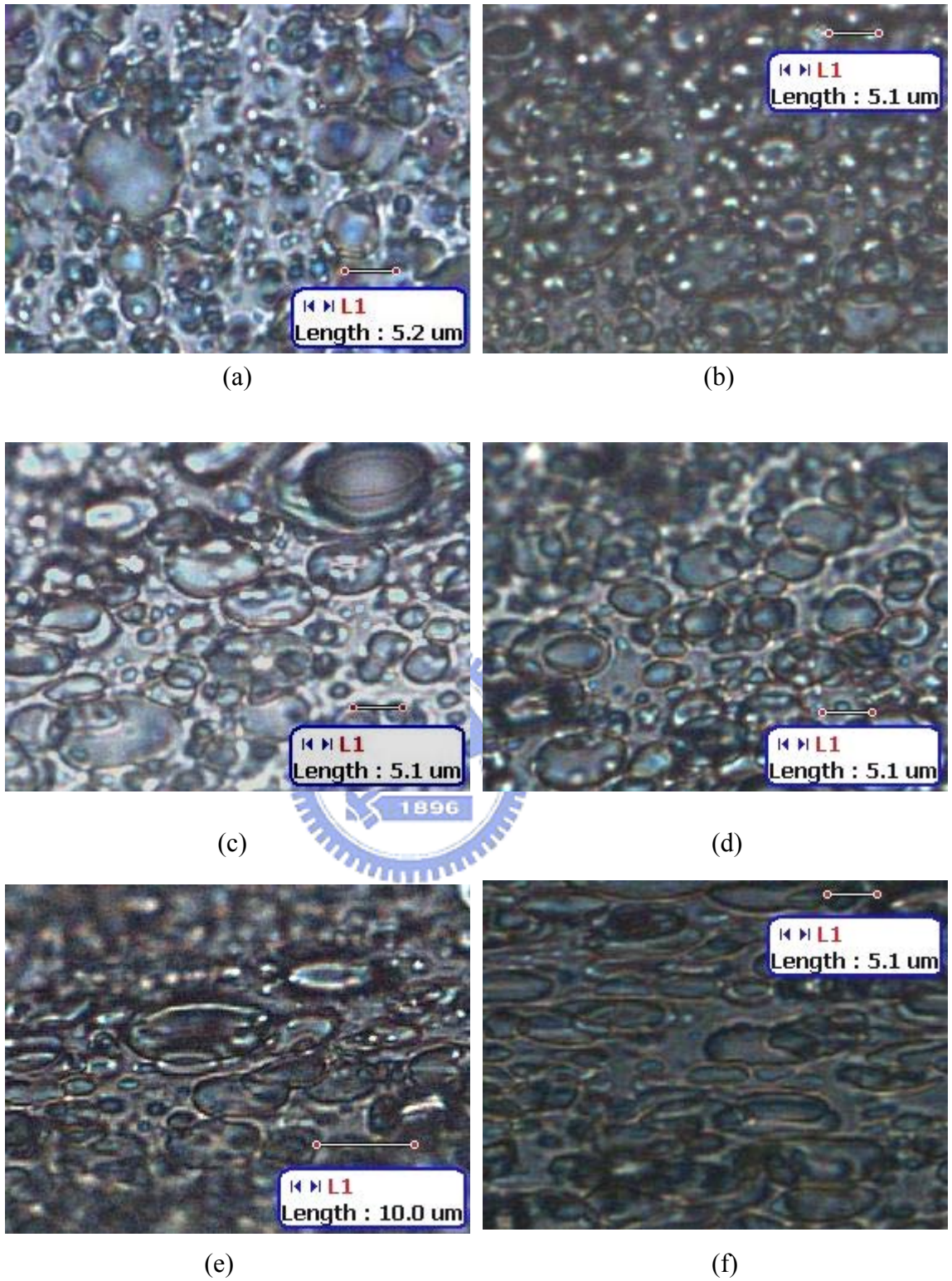


Fig. 31 The PDLC films stretched under the strains of (a) 0% (unstretched) (b) 20% (c) 30% (d) 40% (e) 50% (f) 70%

Tab. 3 Strain and range of deformation of the stretched PDLC films

Strain (%)	Range of deformation
0	1 : 1
20	1.6-2 : 1
30	1.6-2 : 1
40	2 : 1
50	2.5-2.8 : 1
70	3-4 : 1

4.2.2 Dependence of LC Concentration on Optical Properties

The dependence of LC concentration on transmittance under different strain was discussed. The film thickness was fixed at 10 μm in this experiment. The concentration of the liquid crystal (E7) in the PDLC films were adjusted, and the optical transmittances under different strain were measured while the PDLC films were stretched. The measurement results are shown in Fig. 32 where T_{\parallel} and T_{\perp} are the transmittances of the PDLC films, with the parallel and perpendicular polarization state to the stretching direction of the film. When the concentration of E7 was 20 wt%, most of the light transmitted at the normal direction without being scattered by the liquid crystal droplets, and the transmittance was highest among all the samples. The highest T_{\parallel} (50%) was achieved under the strain of 30%. The defects which occurred on the surfaces of the films occasionally due to air bubbles in the films as the strain was higher than 50% would result in intensive and predominantly forward scattering for both \parallel and \perp polarizations and strongly altered T_{\parallel} and T_{\perp} accordingly.

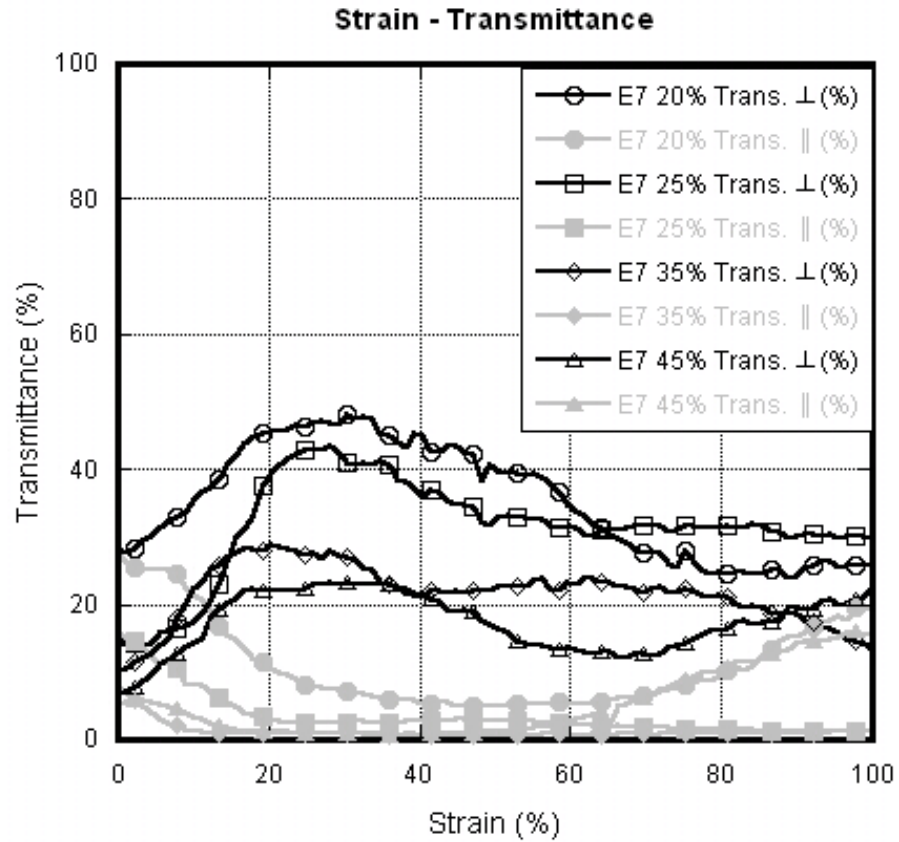


Fig. 32 The strain-transmittance curve of the PDLC films with different concentration of E7

In order to further evaluate the film quality, the extinction ratio was defined as

$$\text{Extinction ratio} = \frac{T_{\perp}}{T_{\parallel}} \quad (15)$$

where T_{\perp} (T_{\perp}) was the transmittance with polarization parallel to the transmission axis, and T_{\parallel} (T_{\parallel}) was the transmittance with polarization perpendicular to the transmission axis. An ideal polarizer has extinction ratio = 0. For real polarizers, extinction ratio is always larger than 0. The extinction ratio properties of the PDLC films with different

concentration of E7 are shown in Fig. 33. The extinction ratio dropped more rapidly as the concentration of E7 was over 25 wt% than it was 20 wt%. When the concentration of E7 was 25-45 wt%, the extinction ratio was lower than 0.1. Thus a sample with the concentration of E7 over 25 wt% had better extinguishing efficiency. Considering both transmittance and extinction, the sample had better performance with 25 wt% of E7.

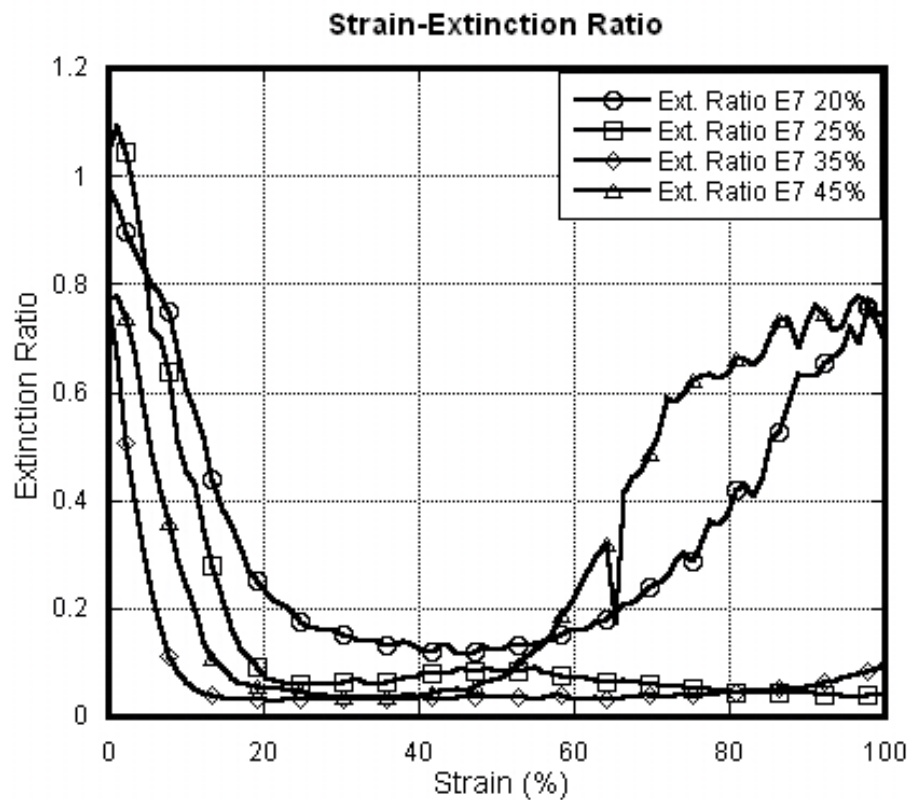


Fig. 33 The extinction ratio properties of the PDLC films with different concentration of E7

4.2.3 Effect of Relative Humidity during Drying Process

The optical performance of the films was unstable when the films are dried in ambient condition. The behavior of the relative humidity which was a parameter of evaporation of water from the film surface was investigated. The concentration of E7 was fixed at 25 wt%. The definition of the relative humidity is the ratio of the partial

pressure of water vapor in air-water mixture to the saturated vapor pressure of water at a prescribed temperature. The relative humidity was controlled while the thin film was dried in the sweatbox. After the film was dried and peeled off from the substrate, the optical transmittance was measured during the stretching process, and the measurement result is shown in Fig. 34 and 35. The transmittance and extinction ratio of the films dried under different relative humidity were almost equal. It can be concluded that only the evaporation rate was steadily controlled by keeping the same relative humidity during the drying process, the optical properties of the film can be kept unison. In the following experiment, 50% of relative humidity was chosen as the experimental parameter since it was close to the environmental condition of the laboratory and easy to be controlled.

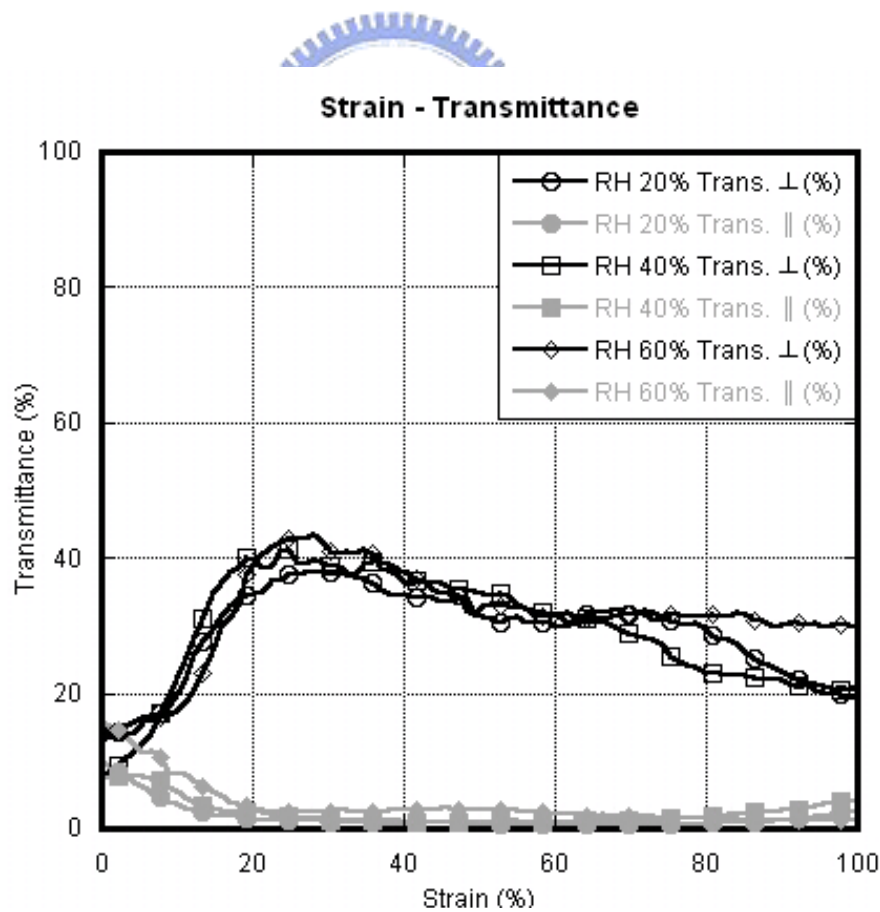


Fig. 34 The strain-transmittance curve of the PDLC films dried under the condition of different relative humidity

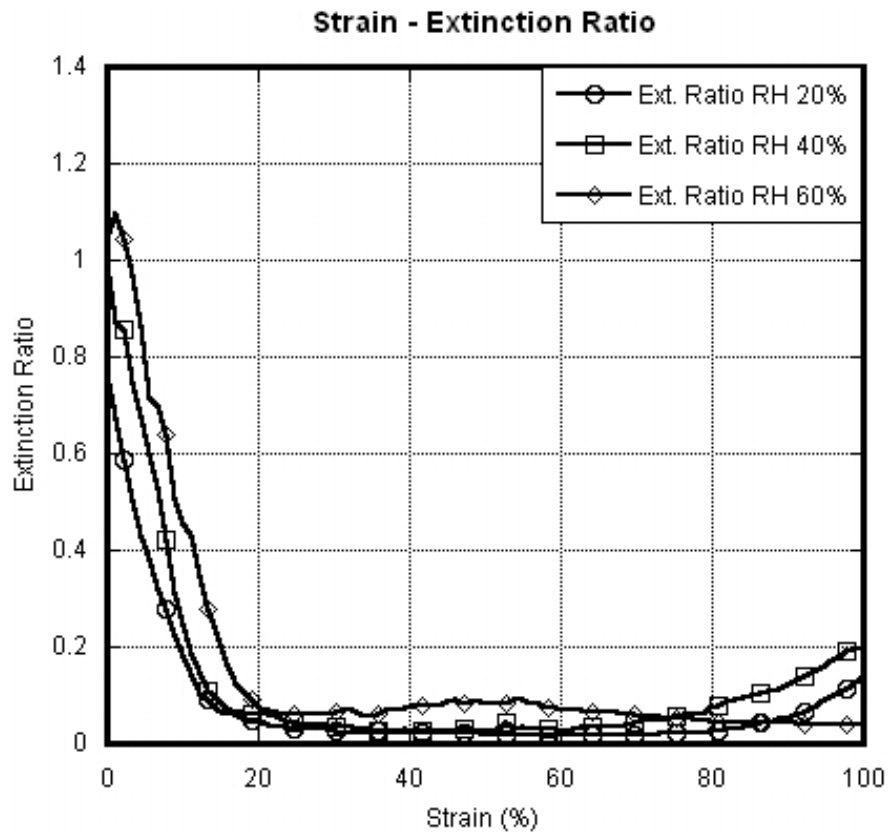


Fig. 35 The extinction ratio properties of the PDLC films dried under the condition of different relative humidity

4.2.4 Dependence of Film Thickness on Optical Properties

The film thickness is an important parameter of transmittance. In this experiment, the film thickness was controlled by the diameter of the stainless wires on the Meyer Bar and had a range of 8-24 μm . The concentration of E7 was fixed at 25 wt%, and the relative humidity was controlled at 50% during drying process. The dependence of film thickness on transmittance and extinction ratio under different strain is shown in Fig. 36 and 37.

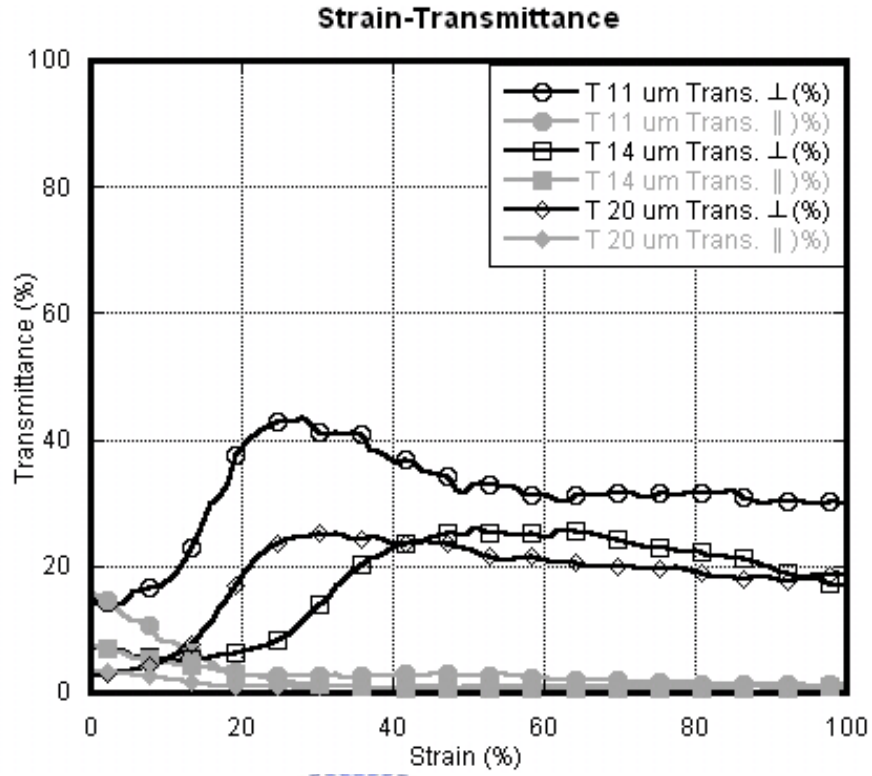


Fig. 36 The strain-transmittance curve of the PDLC films with different film thickness

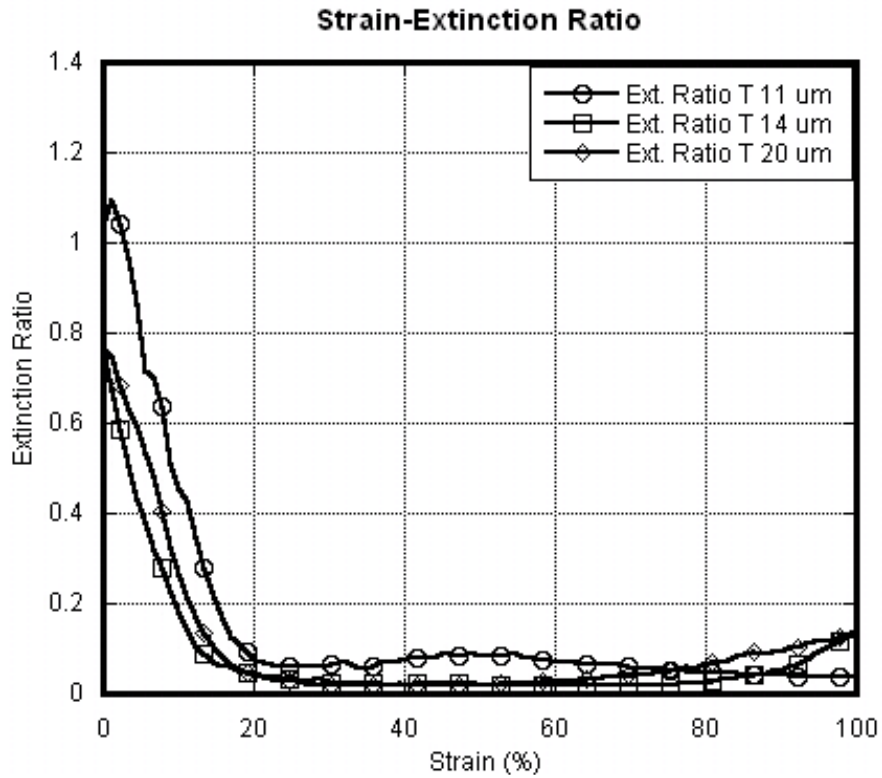


Fig. 37 The extinction ratio properties of the PDLC films with different film thickness

The thinner film had higher transmittance while the extinction ratio was comparable. However, the film will break easily during the stretching process when the film thickness is under 8 μm for our experience. In order to keep robust mechanical property of the stretched film, the thickness of the thin film is supposed to be higher than 8 μm .

4.3 Ordering Parameter of Liquid Crystal

The alignment of liquid crystal molecules in the droplets can be represented by the ordering parameter of liquid crystal which is derived from anisotropic absorption of the representative $\text{C}\equiv\text{N}$ band of E7 as Eq. (14). The incident beam with polarization parallel or perpendicular to the stretching direction of the film was detected by the FT-IR spectrometer, and the absorbance of the $\text{C}\equiv\text{N}$ band of E7 at 2230 cm^{-1} was used to calculate the ordering parameter as shown in Table 4. Since the ordering parameter stopped increasing when the strain arrived at 30%, the alignment of liquid crystal molecules in the droplet had also completed at 30% strain.



Tab. 4 Ordering parameter of liquid crystal under different strain

Strain (%)	A_{\parallel}	A_{\perp}	Ordering Parameter
20%	0.889	0.835	0.0209
30%	0.943	0.853	0.0337
40%	0.937	0.849	0.0335
50%	0.939	0.854	0.0321

4.4 Function of Azimuthal Polarizer

In order to obtain azimuthal polarizers, the fabrication process was extended from one-dimensional linearly stretching to two-dimensional radially stretching. The

concentration of E7 was fixed at 25 wt%, and the film was dried under the relative humidity of 50%. The strain in the radially stretching process is defined as Eq. (16), and the parameters of Eq. (16) are shown in Fig. 38.

$$\text{Strain} = \frac{R' - R}{R} \times 100\% \quad \begin{array}{l} R : \text{Radius of the sample} \\ L : \text{Displacement of the stretching} \end{array} \quad (16)$$

$$R' \approx \sqrt{R^2 + L^2}$$

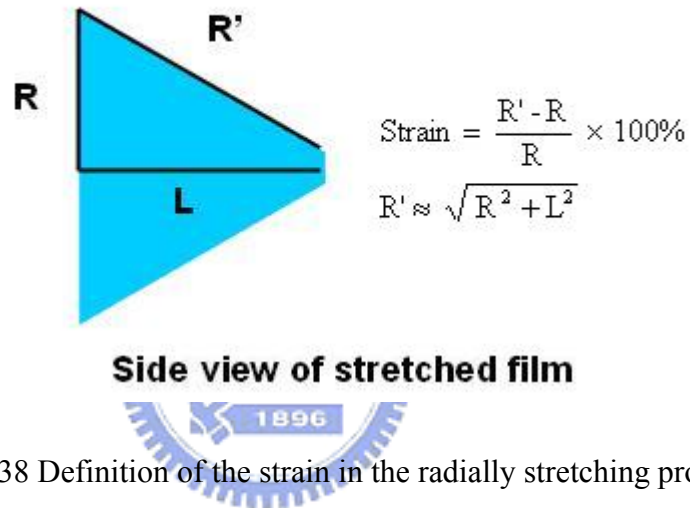


Fig. 38 Definition of the strain in the radially stretching process

The sample was stretched until the strain reach 100% and measured by the polarization testing set-up, as shown in Fig. 39, right after the stretching process. The Helium-Neon (He-Ne) laser operating at 633 nm was used as the light source. The polarization of the incident beam can be controlled to be radial or azimuthal polarization by the radial polarization converter. The incident beam was detected by the CCD camera after passing through the sample. The CCD image appeared in bright state when the incident beam polarized in the azimuthal direction, as shown in Fig. 40. When the incident beam was radially polarized, the CCD image changed from bright state to dark state which proved the function of the azimuthal polarizer achieved by two-dimensional radially stretching.

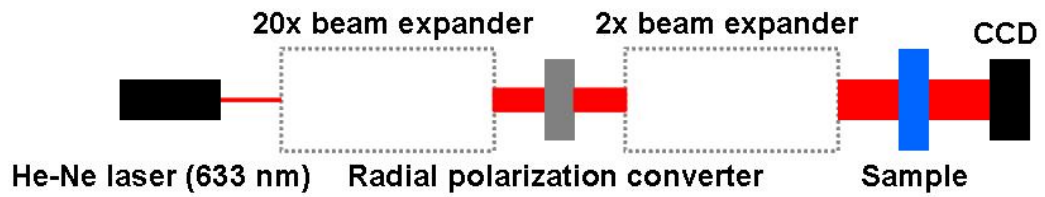


Fig. 39 The polarization testing set-up

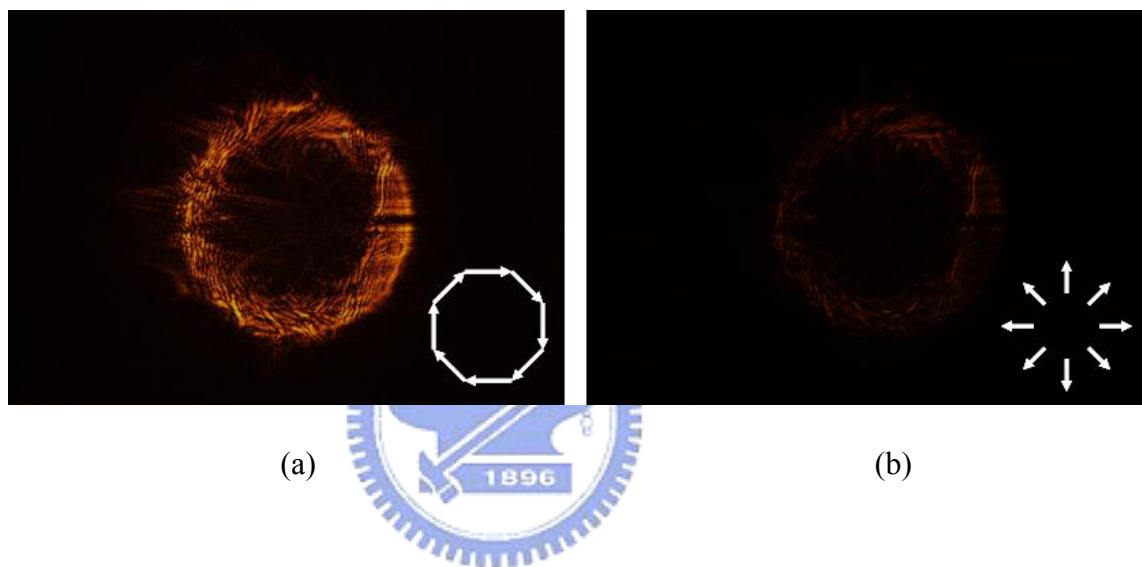


Fig. 40 CCD images with (a) azimuthally polarized (b) radially polarized incident beam

4.5 Discussion

As the measurement results mentioned before, the transmittance at the transmission axis starts to decrease when the strain ratio is over 30% which agrees with the measurement results of the ordering parameter of the liquid crystal. However, the range of deformation of the liquid crystal droplets keeps increasing with the strain ratio. This implies the alignment of the liquid crystal molecules in the liquid crystal droplets has completed at 30% strain ratio, and the effect of the strain arising from the stretching process has saturated.

Besides, the detected highest transmittance at transmission axis is 50% since part of light is scattered to large angle and not detected by the detector located in the normal direction. The light scattering results from the surface roughness of the film, the misalignment of liquid crystal droplets and the existence of the ‘anomalous’ droplets as shown in Fig. 41. Even the film is stretched under high strain, part of liquid crystal droplets are not aligned in the stretching direction which causes the light polarized in the direction of transmission axis to be scattered, as shown in Fig. 41(a). At the same time, the portions of the bipolar configuration in a portion of the droplets do not coincide with the major axis of ellipsoidal cavities. The possible portions of the poles of the bipolar configuration in this case are schematically shown in Fig. 41(b). This kind of liquid crystal droplets also lead to the light scattering to large angle.

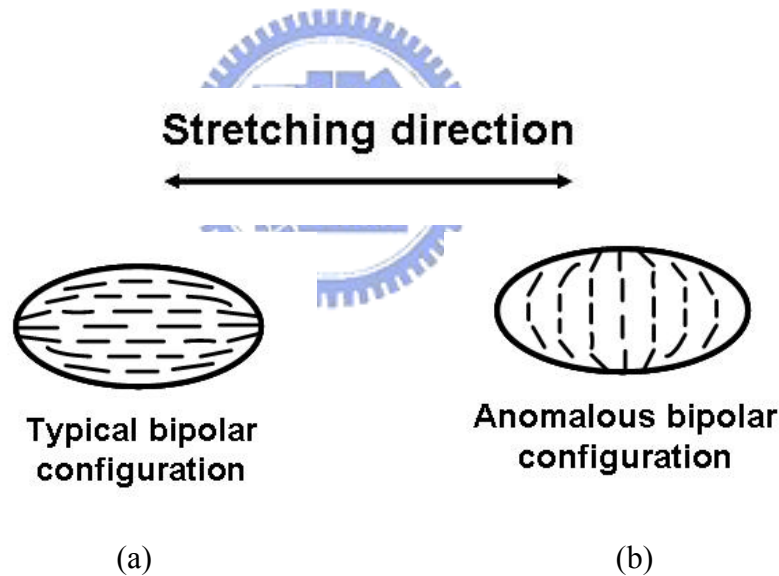


Fig. 41 Schematic representation of (a) the typical orientation of the bipolar director configuration, and (b) the orientation of the bipolar configuration in an ‘anomalous ’ droplet

Chapter 5

Conclusions

5.1 Conclusion

The function of the one-dimensional linearly stretched PDLC films as scattering polarizers has been demonstrated in this thesis. We found that in addition to distortion of droplet shape the polymer orientation during stretching process also contributes to the liquid crystal molecule alignment within the droplets. By simultaneously measuring the strain characteristics and transmittance at transmission or forbidden axis of PDLC films, the relationship between the polarization properties and strain properties of PDLC scattering polarizers has been determined. The film performed 50% transmittance at transmission axis and 0.06 extinction ratio has been demonstrated with determined fabrication parameters as shown in Table 5. Moreover, the azimuthal polarizer can be achieved by 2D radial stretching process. The function of azimuthal polarizers has been demonstrated by the polarization testing set-up.

Tab. 5 Fabrication parameters of stretched PDLC films

Concentration of LC (E7)	25 wt%
Strain ratio	30%
Relative humidity	50%
Thickness of PDLC film	8 μm

5.2 Future Works

The stretched PDLC films which have polarization selectivity can be successfully fabricated by mentioned fabrication process. In order to meet the size of LCDs, the working area of the film will be expanded, and the uniformity should be kept to ensure the optical performance. In order to further control the droplet size which is a key parameter of scattering behavior, the preparation process will be changed to phase separation method instead of encapsulation. The optical properties with oblique incident beam will also be investigated.

The azimuthal polarizers can be achieved by 2D radial stretching. However, the surface roughness is still a key issue to suppress surface scattering. This can be fixed by further improving the fabrication process.



Reference

- [1] I. Amimori, N. V. Priezjev, A. Pelcovits, and G. Crawford, Optomechanical Properties of Stretched Polymer Dispersed Liquid Crystal Films for Scattering Polarizer Applications, *J. Appl. Phys.*, **93**, pp. 3248-3252 (2003).
- [2] R. C. Allen, L. W. Carlson, A. J. Ouder Kirk, M. F. Weber, A. L. Kotz, T. J. Nevitt, C. A. Stover, and B. Majumdar, Brightness Enhancement Film, U. S. Patent No. 6,111,696 (2000).
- [3] E. G. Olczak, M. Yamada, D. J. Coyle, and D. R. Olson, Moiré Free Platform for LCD Backlighting, *SID'06 DIGEST*, pp. 1336-1339 (2006).
- [4] S. Cobb, Jr., B. D. Cull, A. J. Ouder Kirk, M. F. Weber, D. L. Wortman, Diffusely Reflecting Multilayer Polarizers and Mirrors, U. S. Patent No. 5,825,542, .
- [5] 3M (Minnesota Mining & Manufacturing) DBEF Bochure, http://solution.3m.com/wps/portal/3M/en_US/Vikuiti1/BrandProducts/main/productliterature/reflectivepolarizers/
- [6] E. Lueder, *Liquid Crystal Displays* (Wiley, 2001).
- [7] D. Coates, M. J. Goulding, S. Greenfield, J. M. W. Hanmer, E. Jolliffe, S. A. Marden, O. L. Parri, and M. Verrall, New Applications of Liquid Crystals and Liquid Crystal Polymers, *Euro Display'96*, pp. 91-94 (SID, 1996).
- [8] O. A. Aphonin, YU. V. Panina, A. B. Pravdin, and D. A. Yakolev, *Liq. Cryst.*, **15**, pp. 395-407 (1993).
- [9] J. N. Eakin, I. Amimori, and G. P. Crawford, *Proc. SPIE*, **5213**, pp. 283-291 (2003).
- [10] P. Yeh and C. Gu, *Optics of Liquid Crystal Displays* (Wiley, 1999).
- [11] K. Iizuka, *Elements of Photonics* (Wiley, 2002).

- [12] S. C. Tidwell, D. H. Ford, and W. D. Kimura, Transporting and Focusing Radially Polarized Laser Beams, *Opt. Eng.*, **31**, pp. 1527–1531 (1992).
- [13] E. Hecht, *Optics* (Addison Wesley, 2002).
- [14] S. J. Klosowicz, M. Aleksander, and P. Obrzut, *Proc. Of SPIE*, **5947**, 59470M-1-59470M-7 (2005).
- [15] I. Amimori, J. N. Eakin, and G. P. Crawford, *SID'02 DIGEST*, pp. 834-837 (2002).
- [16] S. J. Klosowicz and M. Aleksander, *Opto-Electron. Rev.*, **12**(3), pp. 305-312 (2004).
- [17] Y. Zhao, S. Bai, T. Banh, and J. Brazeau, *Liq. Cryst.*, **27**, pp. 1183-1187 (2000).

